치의과학 박사학위논문

핵인자카파-B 활성화수용체리간드로 유도된 국소적 골다공증을 동반한 비글견 치조골 모델에서 골형성 단백질을 함유한 주사형 베타-삼칼슘인산 미세구의 골형성 효과에 대한 연구

Development of the local osteoporotic alveolar bone of beagle dogs induced by receptor activator of nuclear factor kappa-B ligand and the effect of injectable β-tricalcium phosphate microsphere with bone morphogenetic protein-2 in the osteoporotic alveolar bone

2017년 8월

서울대학교 대학원

치의과학과 구강악안면외과 전공

장 아 렴

핵인자카파-B 활성화수용체리간드로 유도된 국소적 골다공증을 동반한 비글견 치조골 모델에서 골형성 단백질을 함유한 주사형 베타-삼칼슘인산 미세구의 골형성 효과에 대한 연구

지도교수 황 순 정

이 논문을 치의과학 박사학위논문으로 제출함

2017년 4월

서울대학교 대학원

치의과학과 구강악안면외과 전공

장 아 렴

장아렴의 박사학위논문을 인준함

2017년 6월

위 원 장 김명진 (인)

부 위 원 장 황순정 (인)

위 원 명 훈 (인)

위 원 김성민 (인)

위 원 홍종락 (인)

Abstract

Development of the local osteoporotic alveolar bone of beagle dogs induced by receptor activator of nuclear factor kappa-B ligand and the effect of injectable b-tricalcium phosphate microsphere with bone morphogenetic protein-2 in the osteoporotic alveolar bone

Ah Ryum Chang
Department of Oral and Maxillofacial Surgery,
Graduate School of Dentistry
Seoul National University

Background:

Clinical demands of dental implants have been increased for patients with poor bone quality, in whom it is difficult to get a sufficient osseointegration of dental implant even with extended healing time. Enhanced peri-implant bone regeneration in the osteoporotic alveolar bone by sustained release of recombinant human bone morphogenetic protein-2

(rhBMP-2) can increase implant success. In order to achieve such result, a new carrier with optimal release of rhBMP-2 and adequate small size for injectable type is needed. And mandibular alveolar bone of dogs has been regarded as a suitable large animal for bone regeneration research with dental implants and bone substitutes, however, an osteoporotic alveolar bone model of the beagle dog mandible does not exist.

Purpose:

This study aimed to develop a local osteoporotic alveolar bone model on the beagle dog mandible using a local application of RANKL, to evaluate the release kinetics of rhBMP-2 from β-tricalcium phosphate (β-TCP) microspheres and to analyze the effect of a newly developed injectable β-TCP microsphere with rhBMP-2 in this local osteoporotic alveolar bone model of beagle dogs.

Method and material:

To evaluate β-TCP microspheres as a BMP-2 carrier, the release kinetics of BMP-2 was assessed in vitro and was compared with that of collagen sponge and other bone graft materials such as 100% hydroxyapatite (HA) granules, biphasic calcium phosphate granules (70% β-TCP + 30% HA), and 100% TCP granules. For in vivo evaluation, the experimental group was administered the injectable bone graft

material comprising porous β-TCP microspheres and poloxamer hydrogel with rhBMP-2 (45 μg) and the control group was administered the injectable bone graft material without rhBMP-2; the injectable materials were transplanted in non-osteoporotic extraction sockets of both maxillary first molars in four beagles. After 4 weeks, the maxillary alveolar bone was resected to analyze bone regeneration using micro-CT and histomorphometry.

For the development of local osteoporotic alveolar bone, collagen sponges soaked with 0, 20, 40, or 60 μg RANKL were applied into holes created in the mandibular alveolar bone of a beagle dog for two weeks. After the removal of collagen sponges, the bone quality around holes was evaluated with micro-CT to determine the optimal dose of RANKL. After the fabrication of local osteoporosis around five holes in the mandibular alveolar bone of beagle dogs (n = 7) by the application of determined dose of RANKL for two weeks, collagen sponges with RANKL were removed and five dental implants were placed into the holes after the injection of β-TCP microsphere graft materials with four different doses of BMP-2 (0, 5, 15, 45 μg) or without any graft material (control group) in each animal. After four (n = 2) and six weeks (n = 5), animals were sacrificed, and the mandibular alveolar bone was resected to analyze changes of the bone quality at the

outside of inter-thread space and peri-implant bone regeneration within the inter-thread space using micro-CT and histomorphometry.

Results:

Regarding the release kinetics of BMP-2, a significantly more sustained release was observed from porous β-TCP microspheres than from granule bone graft materials ($p < 0.05$) and much more than that observed from collagen sponge after 12 h ($p < 0.001$); the amount of rhBMP-2 released from porous β-TCP microspheres was <21% of the total dose after 26 days. In the maxillary extraction sockets of beagles, the bone volume (BV), BV/tissue volume (BV/TV), and trabecular number were significantly higher in the experimental group than in the control group ($p < 0.05$).

The optimal RANKL dose for the induction of osteoporotic alveolar bone was 40 μg (BV: 41.61% compared to the control). Regarding the bone quality at the outside of the inter-thread space, the BV/TV at 4 weeks was slightly smaller (30.64%) than it immediately after RANKL removal (32.85%). However, the BV/TV and bone mineral density (BMD) were significantly increased at 6 weeks (51.91% and 1.45 mg/cc, respectively) compared to that at 4 weeks (30.64%, 1.36 mg/cc, respectively), which were slight lower to them immediately

after the removal of RANKL (32.85%, 1.37 mg/cc, respectively). In the comparison of the bone quality within inter-thread space between the 4 weeks and the 6 weeks, all micro-CT values at 6 weeks were significantly greater than them at 4 weeks. The BV/TV (12.73%) and BMD (1.27 mg/cc), the BA (40.17%) at 4 weeks were increased to 15.10% and 1.31 mg/cc and 53.03%, respectively at 6 weeks ($p < 0.001$). However, the fold ratio of the increase within the inter-thread space was smaller than it at the outside of the inter-thread space.

In the evaluation of peri-implant bone regeneration, the BV/TV and BMD in all five groups were increased at 6 weeks compared to them at 4 weeks. At 6 weeks, the BV/TV in the group with 5 μg BMP-2 (27.22 %) was the highest among the groups and statistically greater compared with that in the Implant only group (23.14%) and the group with 45 μg BMP-2 (22.97%) ($p <0.05$). The BV/TV in the group with graft material only (26.23%) was statistically higher than that in the Implant only group (23.14%).

In the histomorphometric analysis, the bone area (BA) (%) and bone implant contact (BIC) (%) were the highest in the group with 5 μg BMP-2 (43.80 %, 50.34%, respectively) compared to other groups at 4 weeks. The BA (%) and BIC (%) were significantly higher in the group with graft material only

(51.97%, 58.10%, respectively) and with 5 μg BMP-2 (58.49%, 66.56%, respectively) compared to the Implant only group (44.05%, 50.05%, respectively) at 6 weeks (p <0.05). While there was no significant difference in the BA between the two groups, the group with 5 μg BMP-2 (66.56%) had a significantly higher BIC than that of the group with graft material only (58.10%) (p <0.05) and with 45 μg BMP-2 (52.44%) (p <0.001).

Conclusion:

The new injectable bone graft material comprising porous β-TCP microspheres and poloxamer hydrogels possesses the sustained-release property of rhBMP-2, convenient loading property of BMP-2 using the in situ mixing method, and easy handling for transplantation, which can enhance bone regeneration.

A new beagle dog model for local osteoporotic alveolar bone of mandible was developed using collagen sponges soaked with 40 μg RANKL, which were applied into holes in the alveolar bone for two weeks. In our RANKL-induced osteoporotic alveolar bone, the initial bone quality at the outside of inter-thread space was slightly decreased at 4 weeks after the removal of RANKL, while it was actively increased at 6 weeks. The bone quality within the inter-thread space at 4 weeks was

similar with it immediately after the removal of RANKL, while it was significantly higher at 6 weeks than it at 4 weeks. It seems that the local osteoporotic status in the alveolar bone induced by 40 μg RANKL could be well continued until 4 weeks after the removal of RANKL. And, the new injectable β-TCP microsphere bone grafts could be effectively evaluated with increasing bone formation around the implants, particularly in injectable β-TCP microsphere bone grafts containing 5 μg of BMP-2. However, the bone formation efficacy was not enhanced with increasing BMP-2 concentrations. Our local osteoporotic mandible model of beagle dogs could be useful to evaluate new bone graft materials and implant surfaces to improve bone formation in geriatric patients with osteoporosis.

Keywords: β-TCP microsphere, BMP-2, sustained release, local osteoporotic alveolar bone in beagle dogs, RANKL, peri-implant bone regeneration

Contents

Ⅵ. Reference

Tables

Figures and Figure legends

Abstract in Korea

I. Introduction and literature review

A. Introduction

As the geriatric population has increased, the rate of dental implant demands and the need for surgeries in patients with poor bone quality have increased. Especially, osteoporosis is characterized by the loss of bone mass and density, thereby affecting bone implant contact (BIC) and osseointegration, which can result in increased implant failure (1). In previous animal studies, low BIC and delayed/reduced bone maturation in osteoporotic conditions have been reported (1-6). In a clinical study, patients having osteoporotic conditions did not have optimum bone conditions for osseointegration of dental implants, which is critical for successful dental implant treatment (7). Therefore, to promote peri-implant bone regeneration and improve osseointegration in patients with osteoporosis, ongoing trials have attempted to develop new implant designs and bone substitutes that include recombinant human bone morphogenetic protein-2 (rhBMP-2) (8-10).

rhBMP-2 is one of the most promising options for accelerating new bone regeneration because of its excellent osteoinductivity (11-15). Because rhBMP-2 has an initial burst release, has a short half-life and rapidly diffuses from the application site, supra-physiological doses are required to schieve sufficient bone regeneration (11, 16, 17). However, the

clinical use of high rhBMP-2 doses may contribute to osteoclast activation with elevated ectopic bone formation (18), bone resorption (19-21), cyst-like bone void formation (22), soft tissue swelling (23) and increased cancer risk (24). To minimize adverse effects, more efficient delivery systems for rhBMP-2 have to be developed. A carrier with an optimal release profile may decrease the need for high rhBMP-2 doses (16, 17).

An ideal rhBMP-2 carrier should be able to maximize the efficacy of rhBMP-2 (25). The carrier should efficiently bind to rhBMP-2 and appropriately release it during biological bone formation (25, 26). In addition, the carrier should be resistant to mechanical compression and should function without compromising on surrounding tissues or their molecular biological properties (16, 17, 25). However, no such carrier has been developed yet. Collagen sponge, hydroxyapatite (HA), biphasic calcium phosphate and demineralized bone matrix have all been clinically used as rhBMP-2 carriers (27-29). Collagen sponge is the most widely used carrier of rhBMP-2, however it requires high rhBMP-2 doses due to its weak mechanical strength and initial burst release of growth factor (25, 26). Ceramic materials such as HA and tricalcium phosphate (TCP) are also effective as carriers because of their good osteoconductivity, high affinity to rhBMP-2, and chemical similarity to alveolar bone (30). However, HA may interfere

with further bone remodeling after bone regeneration because of its low absorption rate (16, 17, 31). Therefore, instead of using only HA, it is often combined with TCP, collagen, or other polymers (17). Although the properties of β-TCP are similar to those of HA, β-TCP has the advantages of complete resorption and better osteoconductivity (32); therefore, it has attracted attention as a carrier of rhBMP-2. β-TCP can be used in the form of the block, particles/granules, or microspheres. The particle size of β-TCP microspheres (45-75 μm) is smaller than that of granule-type β-TCP (0.5-2.0 mm), enabling a higher penetration in the surrounding trabecular bone spaces and a more effective filling of the narrow gap between the implant and surrounding bone. Because the surface area of β-TCP microspheres is larger than that of block- or granule-type β-TCPs, rhBMP-2 binding sites can be increased and a more sustained release effect can be expected. However, the release pattern of rhBMP-2 from β-TCP microspheres has not yet been reported.

Injectable carriers offer several advantages, such as the ease of handling and the ability to fill a desired shape, reduce voids between dental implant and bone substitutes, and improve the contact between the carrier and dental implant surface (31, 33, 34). In addition, it is easier to incorporate rhBMP-2 in injectable carriers than in particulate-type carriers. Injectable carriers usually comprise hydrogel, either alone or in

combination with a particulate- or microgranule-type carrier. Among various hydrogels, such as hyaluronic acid (8, 34, 98, 152), chitosan (31, 151) and collagen hydrogels (35,36), poloxamer hydrogel (33) is attractive as a carrier for rhBMP-2 due to its high water content, which contributes to high biocompatibility and protein-loading capacity (33, 37, 38). Further, it has thermo-reversible properties; it forms a gel-like composite at room temperature to promote the solubilization of weakly water-soluble drugs and assumes a gel state at body temperature (38). Therefore, injectable composite carriers composed mainly of porous β-TCP microspheres and poloxamer hydrogels may be an improved delivery system for rhBMP-2. However, its effect on bone regeneration has not been reported.

The most widely used osteoporotic animal models are ovariectomized (OVX) rats (3-5). However, the rat mandible is too small to place dental implants. Moreover, bone metabolism of rats is quite different from that of humans because their bone structure lacks the Haversian system (39, 40) and has a microstructure different from that of human (39, 40). The bone of dogs is the most similar to that of human (41) and has the Haversian system and a basic multicellular unit (BMU)-based remodeling system (39-41), making it suitable for dental implant research. However, previous studies have shown inconclusive results on the effects of ovariectomy in

dogs (42–45). Drezner and Nesbitt (1990) reported a decrease of vertebral bone density by 8–10% at 8–12 months after ovariectomy in beagles (45), but many other studies have reported that bone loss in OVX dogs is insignificant (42–45), because the estrogen level is always kept low due to the infrequent estrus cycle (twice a year) in dogs (40). Therefore, for making an osteoporotic beagle dog mandible model, different methods other than OVX are needed.

Receptor activator of nuclear factor kappa–B ligand (RANKL) is known as the final effector of osteoclastogenesis and bone resorption (46). Recently, studies have targeted osteoclasts by activating or blocking the RANK/RANKL signal pathway, which leads to the promotion or inhibition of bone resorption, have been conducted (46–55). This concept can be utilized to make osteoporotic models. RANKL is widely used for *in vitro* induction of osteoclastogenesis and is also used in animal experiments. Tomimori et al. (2009) reported that rats systemically injected with RANKL showed rapid bone loss and decreased bone mineral density (BMD) and that there was no significant difference compared with the OVX model (56). In the studies with locally applied RANKL, active osteoclasts were induced and bone resorption was observed (57, 58). However, models of locally induced osteoporosis by RANKL have not been reported in dogs. Therefore, it is necessary to develop a local osteoporotic alveolar bone model of dogs using a local

application of RANKL. This model was created by applying collagen-absorbed RANKL directly to the mandible of a beagle for two weeks.

B. Literature review

1. BMP

1.1. History and property of BMP

BMPs are a group of growth factors also known as cytokines and metabologens (59). In 1965, the activity of BMPs was first identified by Urist (14). He discovered a substance in the extracellular bone matrix that could induce osteogenesis when implanted in extra skeletal soft tissue (14). Studies on the purification of bone morphogenic proteins by the Reddi (59) and replication of BMPs by John Wozney (60) have made considerable progress in BMP studies.

Bone induction is a sequential multistep cascade. The key steps in this cascade are chemotaxis, mitosis, and differentiation. The sequence of these events involved in bone matrix-induced bone morphogenesis was unraveled by Hari Reddi (59). Specifically, BMPs may trigger the migration of mesenchymal stem cells; then, subsequent cell proliferation is activated. Next, initiation of chondroblast differentiation occurs, and finally, cartilage tissue is formed and calcified by concomitant angiogenesis and vascular invasion, thus leading to completion of bone formation (59).

To date, 20 types of BMPs have been discovered; however, only BMP-2 to BMP-7 are reported to be osteoinductive (61).

They are further divided into subfamilies according to their amino acid sequence similarities. BMP-2 and BMP-4 form the first subgroup, BMP-5 and BMP-7 form the second, and BMP-3 forms the third (62). Mayer et al. (1996) suggested that different BMPs vary in their mitogenic capacity (63). However, there are several conflicting results regarding the osteogenic effect of different BMPs (63, 64).

Although several BMPs have osteogenic properties (65), rhBMP-2 was the first to be introduced as a bone graft substitute. It was first introduced in the United States in 2002 with the approval of the Food and Drug Administration (FDA) for single-level anterior lumbar interbody fusion (ALIF)(20, 66). Then, BMP-2 was approved for use in open tibial surgery in 2004 (67). In terms of oral and maxillofacial reconstruction, rhBMP-2 was approved in 2007 for sinus augmentation and localized alveolar ridge augmentation.

1.2. BMP-2 signaling

BMP signaling translocation begins when BMP binds to BMP receptor types I and II whose signal is regulated by phosphorylation of receptor-regulated R-Smad (typically Smad 1, 5 and 8)(68). Phosphorylated R-Smad forms a heterodimeric complex with Co-Smad (typically Smad 4) and perpetuates the signal to translocate into the nucleus to direct the transcriptional response (69, 70).

The cellular effect of BMP-2 is more pleiotropic than molecular signal propagation. In fact, BMP-2 activates peroxisome proliferator-activated receptor γ (PPARγ) signaling (71), which induces adipogenic differentiation and fat formation (72). BMP-2 also induces a number of inflammatory cytokines and chemokines, including interleukin (ILs), and tumor necrosis factor (TNF) $-\alpha$ (73). It is also well known that BMP-2 activates osteoclasts through RANKL (74). It has been shown that BMP-2 causes clinically relevant adverse effects due to different effects with adipogenesis, inflammation, and osteoclast activation (75).

Especially, current literature suggests that BMP-2 directly influences the formation and activity of osteoclast through Smad signaling (76, 77), and indirectly promotes osteoclast through enhanced expression of osteoclastic-promoting factors, such as RANKL, produced by osteoblasts (78). As the enhanced expression of osteoclast differentiation genes by BMP-2 was dependent on RANKL. BMP-2 was unable to induce osteoclast differentiation in the absence of RANKL (76).

1.3. BMP-2 dose in clinical use

BMP-2 has species-specific concentration requirements for osteogenesis (75). Thus, the BMP-2 concentration necessary for inducing consistent bone formation is substantially higher in nonhuman primates (0.75–2.0 mg/mL) than in rodents (0.02–

0.4 mg/mL) (75). This may be due to the requirement of a higher number of responding cells in larger animal. The FDA-approved concentrations of 1.5 mg/mL BMP-2 for human use have been determined by non-human primate efficacy tests (19) (75).

The dose-dependent efficacy in humans was observed in fracture healing studies and the healing time decreased with 1.50 mg/mL BMP-2 but not with 0.75 mg/mL BMP-2 (79). Since effective bone treatment in humans requires large amounts of BMP-2, the incidence of adverse effects increases as well. In fact, excessive concentrations of BMP-2 may be the most important cause of most adverse effects (80).

Therefore, various clinical trials have been conducted to determine the optimal dosage of BMP-2(81). In clinical studies of the dental field, the dose efficacy of rhBMP-2 in patients requiring extraction socket augmentation was investigated and it was found that the bone regeneration effect was higher in the 1.5 mg/mL group than in the 0.75mg/mL group (27). In another study, although 0.43 mg/mL rhBMP-2 was found to be effective in bone induction in sinus floor elevation study, but 1.5 mg/mL rhBMP-2 showed the highest efficacy for bone induction (82, 83).

1.4. Clinical adverse effects

In clinical use, the most common adverse effect of BMP-2 is

seroma formation encountered commonly in the first week after surgery (84, 85). Patients with cervical spine swelling and throat tissues complained of dysphagia and difficulty breathing or speaking. (86). Second, the most recognized adverse effect is ectopic bone formation associated with the leakage of BMP-2 outside the implant site. Ectopic bone formation is estimated to occur approximately six times more in BMP-2 applied patients than in control patients (18). Third, one of the adverse effects of spinal surgery is osteolysis, which occurs because of increased BMP-2 dosage (12 mg-18 mg). Disc displacement, osteolytic lesions, and implant displacement occurred more in the BMP-2 group than in the control group (21, 66). However, this adverse effect seems to be transient. Because, these radiolucent areas were not seen on computed tomography (CT) scans at 24 months (21, 66). Another adverse effect is cyst-like bone formation. Although there are no clinical reports of bone cyst formation in the patient., it has been previously reported in *in vivo* preclinical studies (87). Previous studies have shown the increased spacing of trabecular bone along with interspersed lipid deposition close to the site of BMP-2 implantation, resulting in cystic bone formation (87, 88). Finally, the role of BMP-2 in the carcinogenesis is controversial. However, abnormal physiological expression of BMP-2 is clearly associated with several tumor types (24). The biological significance of BMPs in various cancers raises the potential concerns regarding clinical use of BMP-2.

1.5. Methods to improve BMP-2 use

With the accumulation of clinical experience with BMP-2, several potential adverse effects have been identified, and much effort has gone into finding safer and more effective alternatives to BMP-2. To date, no suitable alternative to BMP-2 with similar or superior bone inducing properties but lesser adverse effects has been found. Therefore, to minimize adverse effects of BMP-2, several studies have investigated its appropriate dosage, scaffold and the supplemental proteins or growth factors (75).

Recent study suggests that there is cross talk between VEGF and BMP signaling pathways (89). When combined with BMP-2, VEGF exerts synergistic effects in rat model, increasing the advancing complete healing of the defect (90). However, the combined use of BMP-2 and VEGF may cause abnormal migration of BMP-2 to unwanted regions, and may lead to ectopic bone formation (91). One of the many concerns about the use of BMP-2 is the potential for BMP-2 activation in osteoclasts.

Bisphosphonates prevent bone loss and are clinically suitable for the treatment of osteoporosis (92). The use of bisphosphonates with BMP-2 has been shown to significantly reduce the number of osteoclasts on bone surface area. This can avoid extreme bone loss associated with BMP-2, which can lead to osteolysis. Conversely, when osteoclasts are decreased,

the differentiation and function of osteoblasts are much less regulated and adverse effects such as ectopic bone formation, become more frequent than observed in treatment with BMP-2 alone (75).

Supra-physiological dosage of BMP-2 causes a large inflammatory response. Major cytokines IL-6, IL-10, and TNF-α highlight the proinflammatory conditions induced locally by BMP-2 (93). The administration of adjunctive corticosteroids with BMP-2 relates to the reduce inflammatory response induced by BMP-2 (94).

Because of the burst release, short half-life and rapid diffusion of rhBMP-2 from the site of application [8, 150-154], various carrier materials for sustained release of rhBMP-2 have been introduced. However, an ideal BMP-2 delivery system has not been established. Collagen sponge is the most widely used carrier approved by the FDA. In many previous studies, collagen sponge showed successful clinical results in accelerated healing and excellent bone regeneration. (79, 95). However, collagen use reportedly has problems with compressibility, growth factor retention, bone formation outside the target area, and the requirement for large doses of rhBMP-2 (96). Therefore, alternative carriers of BMP-2 are being developed and are described in detail below.

2. BMP-2 carriers for sustained release

In clinical rhBMP-2 treatment, regulation of the release rate of rhBMP-2 to the target site has been studied to achieve higher efficacy of rhBMP-2 for bone regeneration (25, 26). Uludag et al. reported that carriers with differences in pharmacokinetics have different release and retention rates of BMP-2 (97). Winn et al. reported that the release kinetics of the delivery system can have a crucial influence on the clinical effects of BMP-2 (98). The osteoinductive effect of rhBMP-2 may also be influenced by the release rate of the carrier (99, 100). The osteogenic response can be promoted more effectively by being gradually released from a specific scaffold [55].

2.1. Hyaluronic acid

Hyaluronic acid and its derivatives have been extensively studied in biomedical and tissue engineering applications such as gels, sponges, and pads and as viscous gels which are percutaneously injected in ophthalmic surgery (101). Hyaluronic acid also has an osteoinductive effect, and bone formation in mandibular defects is better with hyaluronic acid than with collagen sponges when both carriers are used to deliver BMP-2 in rats as well as in human clinical trials (102). This is because hyaluronic acid based delivery vehicles retain more BMPs than collagen sponges (98). Hyaluronic acid enhances alkaline phosphatase (ALP) activity, and actively

interact with BMP to produce direct and specific cellular effects. However, such a hydrogel- type carrier lacks mechanical strength to be used alone.

2.2. Synthetic biodegradable polymeric carriers

Unlike natural polymers and collagen, synthetic biodegradable polymers do not carry the risk of immunogenicity or disease transmission. The sustained delivery of BMP-2 through the poly lactic-co-glycolic acid (PLGA) microsphere system also resulted in greater bone healing (103). For more effective bone regeneration, these scaffold systems can be conjugated with specific factors that can regulate the release rate of target molecules (104). These carrier systems with specific factors reported to induce new bone formation with a small amount of BMP-2 loaded. For example, PLGA/polyethylene glycol (PEG) scaffolds induced an increase in new bone volume by loading with 1-μg BMP-2 (104). Heparin-conjugated PLGA scaffold also enhanced the osteogenic effect of BMP-2 by sustained release of 1 μg BMP-2 (105).

2.3. Hydroxyapatite

Hydroxyapatite (HA) is well known for its osteoconductivity and has been widely used clinically as a bone substitute since the 1970s due to its ability to bind directly to the bone (106).

Synthetic HAs are provided in ceramic (porous and non-porous) forms (107) where only porous HAs are evaluated as scaffold and controlled release carriers (particles, powders, granules, discs or blocks) of BMPs for bone regeneration (101).

However, bone induction is insufficient due to lack of absorption and the high affinity between the substance and the BMP. Therefore, HA binds with tricalcium phosphate, collagen, and other natural and synthetic polymers. These composites exhibited superior local BMP delivery and bone formation than HA alone *in vivo*. (108, 109).

2.4. Tricalcium phosphate

Tricalcium phosphate (TCP) was one of the earliest calcium phosphate compounds to be used as a bone graft substitute. In 1920 Albee and Morrison reported that the rate of bone union was increased when TCP was injected into the gap of a segmental bone defect (110). β-TCP is available in porous or solid form as either granules or blocks. Structurally porous β-TCP has compressive and tensile strengths similar to those of cancellous bone (111). Like other calcium phosphates, it is brittle and weak under tension and shear but is resistant to compressive loads (112). Typically, it has been used in its granular porous form. Porous granules tend to migrate less than solid granules due to earlier fixation by fibrovascular ingrowth (113). β-TCP undergoes resorption over a 6-12 month period without adverse effects (114, 115), and then,

replacement of β-TCP by bone occurs (116).

However, there are some disadvantages to β-TCP. First, the absorption is not completely consistent with the new bone formation. In general, resorption happens slightly faster than new bone formation (117). Second, it has poor mechanical properties, such as brittleness, inability to resist fatigue and insufficient holding power (118); these restrains its application in weight-bearing areas (119). To overcome the disadvantages of β-TCP and improve its biological and physical properties, some bone regeneration materials have been used with it to form composites. These bone substitute materials include a bone inductive material (BMP-2), platelet rich plasma (PRP) and bone conduction materials (PGLA and HA).

In the case of β-TCP and BMP composites, β-TCP as a carrier can prolong the action time of BMP, while BMP can complement osteoconductivity of β-TCP and promote new bone formation. Urist et al. (120) reported that β-TCP could stimulate the biological activity of BMP, since the new bone mass formed with β-TCP and BMP composite (1 mg) is 12 times higher than that of BMP alone. Dohzono et al. (121) found a large osteoclast cell containing BMP-2 on the surface of the β-TCP scaffold. In other words, BMP can accelerate the degradation of β-TCP scaffolds, thus providing sufficient space for new bone formation and remodeling. Ohyama et

al.(122) found that dogs treated with β-TCP and BMP composites showed better interbody fusion rates and mechanical strength, and more bone trabecula in posterior lumbar fusion than untreated dogs or those treated with β-TCP alone or autografts. In addition, β-TCP blocks the invasion of surrounding soft tissues, thereby providing favorable conditions for osteogenesis. Besides prolonging the release of BMP, β-TCP may also activate BMP-2 (123). In terms of mechanical properties, β-TCP provides better stability than collagen sponge by resisting compression from surrounding soft tissue (124).

3. Osteoporotic animal model

Animal models are essential to demonstrate the benefits of a new approach that is completely different from standard treatments. In addition, preclinical testing of new therapies or devices is required to demonstrate efficacy and safety. According to preclinical and clinical evaluation guidelines for drugs used to treat or prevent postmenopausal osteoporosis, the US Food and Drug Administration (FDA) recommends that the agents be evaluated in two different animal species, including OVX rats and a large, non-rodent animal that possesses Haversian systems and remodeling patterns similar to those of humans (39). Therefore, the need for large and small animal models with osteoporosis is evident because

preclinical evaluation of new clinical treatment options is required (125).

Osteoporosis occurs naturally only in human and non-human primates. Cerroni et al. reported that the pattern of skeletal maturation in rhesus monkey is similar to that in human females (126). This pattern includes an age-dependent decrease in spinal BMD. This is the only report on naturally occurring osteoporosis and spontaneous fractures in animals. Osteoporosis does not naturally occur in other animals and thus needs to be induced in the experimental environment (125).

3.1. Induction of osteoporosis

3.1.1. Ovariectomy

Ovariectomized rats are the most studied the animal model for osteoporosis. This model mimics postmenopausal cancellous bone loss in humans when examined over relatively short periods of time. However, this model is limited by the lack of the Haversian system in cortical bone and the absence of impaired osteoblast function during the late stages of estrogen deficiency and that of multicellular unit-based remodeling in young rats (125). In addition, the size of the rodent, while advantageous in terms of housing, is unfavorable for orthopedic procedures and dental implant surgery.

Dogs are the most controversial model. The obvious

advantage of dogs in the study of osteoporosis is that they possess cortical bone with a Haversian system and manifest internal cortical and cancellous bone remodeling processes similar to those in humans. In several studies evaluating the effects of ovariectomy in dog, cancellous bone volume was shown to be either decreased (43, 127) or unchanged (42, 44). Ovariectomy in dogs does not induce osteoporosis because estrogen level always kept low due to the infrequent estrus cycle (twice a year) in dogs (40). Although the results appear to be heterogeneous, OVX dogs seem inappropriate as a model for studying bone loss following ovariectomy (128).

3.1.2. Diet

In previous study, osteopenia has been studied after administration of low-calcium diet to immature rats (129). The effects of dietary magnesium supplementation and the calcium/phosphorus ratio in food have also been investigated in the rat model of ovariectomy-induced osteoporosis (130, 131). Spencer et al. reported osteoporotic bone loss in female swine kept on a calcium- and phosphorus-restricted diet starting at seven weeks of age. After six weeks of this diet, these swine showed osteopenia (132).

3.1.3. Drugs

Drugs, particularly corticosteroids, alter bone metabolism and to induce osteoporosis by decreasing bone formation and

bone mass. Ovariectomized sheep treated by steroids and fed a calcium or vitamin D-restricted diet showed a decrease in BMD (133). It is known that glucocorticoid-induced osteoporosis differs from postmenopausal or senile osteoporosis. However, to study the aspects f implant fixation, animal models using glucocorticoid-induced osteoporosis emulated the human situation. The decrease of BMD after ovariectomy is more pronounced with steroid medication administration than without (134).

3.1.4. Immobilization

Most studies of immobilization reported significant reductions in mineralization and histomorphometric parameters of osteoporosis. Unlike osteoporosis, immobilization presents with locally apparent bone loss (125, 135).

3.1.5. Central control of bone mass

Besides the known critically important local regulation of bone remodeling, recent genetic studies have reported a central control of bone formation that might be used to induce osteoporosis in animal experiments. This central regulation involves leptin and the sympathetic nervous system (136). Knockout mice missing the gene coding for leptin have a massive increase in bone mass (137).

3.2. Osteoporotic model of dogs

Dogs are one of the more frequently used large animal species for musculoskeletal and dental research. A study by Aerssens et al. (1998) investigated the differences in bone composition, density and quality between various species (human, dog, sheep, pig, cow and chicken) (41) and found that the bone composition between dogs and humans showed the highest similarity in terms of ash weight, hydroxyproline, extractable proteins, and IGF−1 content. In terms of bone density, dogs and pigs showed the highest similarity to humans. Overall, the authors concluded that dogs best reflect the characteristics of human bones (41). These results are also supported by earlier findings of Gong et al. (1964), wherein human and dog cortical and cancellous bones were found to have similar water fraction, organic fraction, volatile inorganic fraction, and ash fraction (138).

However, due to ethical concerns associated with inducing osteoporosis after ovariectomy in dogs and their status of a companion animal, the use of dogs in medical research is being contested. Another problem is the difference in the rate of bone remodeling between the species (39). This is important as implant−associated changes that may be evident in a dog model may not be as apparent in humans, owing to the lower remodeling rate in the latter (139). Although there are structural similarities in trabecular bone turnover between dogs and humans (140), there is a large variation in trabecular bone

turnover between individual (39). Therefore, in a dental research using dogs, inter-individual differences in measurements may be considerable.

C. Experimental purpose in brief

First, we herein evaluated the release kinetics of rhBMP-2 from β-TCP microspheres *in vitro* and the bone regeneration effect in non-osteoporotic extraction sockets of the beagle dog maxilla. Second, we developed a local osteoporotic alveolar bone of the beagle dog mandible by locally applying RANKL. The consequent changes of bone quality were evaluated immediately after and four and six weeks after RANKL removal. Finally, we evaluated peri-implant bone regeneration by injectable β-TCP bone grafts with different doses of rhBMP-2 on the local osteoporotic alveolar bone of the beagle dog mandible at four and six weeks after implant placement.

Ⅱ. Materials and Methods

1. Evaluation of injectable β-TCP microspheres combined with rhBMP-2

1.1. Release pattern of rhBMP-2 in vitro

Preparation of porous β-TCP microspheres

The porous β-TCP microspheres were provided from Bioalpha Inc (Seongnam, Korea). They were prepared by the spray-dry method (67). These particles were sintered at 1,050 ℃ for 2 h, resulting in diameters ranging from 45 to 75 μm and porosity of 68 % (Figure 1A).

rhBMP-2 loading and release kinetics

Four different carriers [Collagen (Dalim Tissen Co. Ltd., Seoul, Korea), 100% HA granule (Bioalpha Inc, Seongnam, Korea), biphasic calcium phosphate granule (70% β-TCP + 30% HA; Cowellmedi Co., Busan, Korea), 100% β-TCP granule (Bioalpha Inc, Seongnam, Korea)] were prepared to evaluate the release kinetics of rhBMP-2. Porous β-TCP microspheres (Bioalpha Inc, Seongnam, Korea) and the abovementioned four carriers (n = 4 for each carrier) were separately placed in a 24-well plate, and 5 μg of rhBMP-2 (*Escherichia coli*-derived rhBMP-2; CGBio, Seongnam, Korea) was added to each well. The rhBMP-2 solution was evenly

distributed over the surfaces using a micropipette, and the plates were incubated for 30 min at room temperature.

To evaluate the release kinetics of rhBMP-2 in vitro, all samples were immersed in 1 mL of elution buffer (phosphate-buffered saline containing 1% bovine serum albumin). The supernatant was collected at various time points (1 and 12 h and 1, 2, 5, 12, 19, and 26 days), and the plates were replenished with 1 mL of fresh buffer. The amount of released rhBMP-2 was quantified using the human BMP-2 "Super X" ELISA kit (Antigenix America Inc., NY, USA), as per the manufacturer's instructions.

1.2. Alveolar bone regeneration in non-osteoporotic maxillary extraction sockets of the beagle dog maxilla

Preparation of injectable β-TCP bone graft materials

A mixture of porous β-TCP microspheres and 35 wt% poloxamer 407 hydrogel was prepared as the injectable bone graft material (ExcelOS Inject®, Bioalpha Inc., Seongnam, Korea) (Figure 1B). rhBMP-2-loaded injectable bone graft material was prepared by the in situ mixing method, wherein one syringe containing the injectable β-TCP and another containing rhBMP-2 solution were interconnected via a two-way connector; 20 piston movement cycles of each syringe were performed to ensure homogeneous mixing. For this

experiment, injectable β-TCP microspores with 45 μg rhBMP were used for the experimental group.

Surgical procedure

Four beagles (age, 3 years; weight, 12-13 kg) were used in this study. The experiment was approved by the institutional Animal Care and Use Committee, School of Dentistry, Seoul National University. All surgical procedures were aseptically performed under sedation with Zoletil 50 (0.05 mg/kg; Virbac S.A., Carros-France) and Rompun (0.15 ml/kg; Bayer Corp., Korea). Marginal gingiva incisions were made in the maxillary first molar region. Both first molar teeth were carefully extracted without fracturing the socket walls. We prepared a mixture of 0.5 cc injectable β-TCP microspores and rhBMP-2 (45 μg/0.1 cc) for the experimental group and a mixture of 0.5 cc injectable β-TCP microspores and 0.1 cc sterile water for the control group and transplanted the graft material in the fresh extraction sockets. A mucoperiosteal flap on the buccal side was elevated and covered the socket entrance. The wound was carefully sutured. After 4 weeks, the dogs were killed with an excess of ketamine, and via carotid arteries, a fixative containing a mixture of 5% glutaraldehyde and 4% formaldehyde was perfused. The maxilla was excised and placed in the fixative. Each surgical site in the first molar area was resected.

Micro-CT analysis

All specimens were scanned using a SkyScan 1172 Microfocus CT system (Bruker micro-CT, Kontich, Belgium) with a resolution of 17 μm. Three-dimensional scans were taken at an X-ray energy level of 80 kV and a current of 124 μA. The collected images were 1000 × 524 pixels in size. Micro-CT scans were taken to quantitatively evaluate new bone formation using the SkyScan 1172 Microfocus X-ray System (SkyScan) and the CT software, including CTAn 1.8, CTvol, and NRecon Reconstruction®.

To measure the newly formed bone, a predefined size (ø3mm) was selected as the region of interest (ROI) in two-dimensional images at the palatal root socket. The pixel zone representing ossification in the defined ROI was then three-dimensionally reconstructed by creating a volume of interest (VOI). Each VOI was 3 mm in diameter and approximately 3.5 mm in height including 200 slices from the alveolar crest. Using the CTAn 1.8 software program for each reconstructed BMP file, bone volume (BV), tissue volume (TV), BV/TV ratio, trabecular number (Tb.N), trabecular thickness (Tb.Th), and trabecular space (Tb.Sp) were obtained.

Histomorphological analysis

Specimens were fixed in 10% buffered neutral formalin for 1 week, bone blocks were dehydrated, and decalcified sections were embedded in methylmethacrylatein; approximately 5 μm-thick embedded sections were cut. The sections were

stained with hematoxylin and eosin. Digital images of the stained sections were obtained using the Olympus BX51 Microscope (Olympus, Tokyo, Japan) equipped with a digital camera (SPOT Insight, Diagnostic Instrument, Inc., Sterling Heights, MI, USA). The percentage of BA (%) was determined using the Image J software (National Institutes of Health, Bethesda, MD, USA).

2. Development of a local osteoporotic alveolar bone model on the beagle dog mandible

2.1. Evaluation of local osteoporosis induced by RANKL in the alveolar bone set-up model

Set-up of a local osteoporotic beagle dog mandible model induced by RANKL

The study protocol was approved by the Institutional Review Board of Seoul National University Dental Hospital (approval no. CRI05008) and was conducted in accordance with the legal regulations for investigations of human tissue and organs in South Korea. For confirmation of the rate and level of bone resorption by RANKL, holes with 4-mm depth were made by a 3-mm diameter trephine bur on the mandible of a 1-year-old beagle (weight, 12-13 kg), and bone resorption was induced by the application of a collagen sponge that had absorbed RANKL before being implanted into the hole and leaving for two weeks.

RANKL in different concentrations (20, 40, and 60 μg) was absorbed into the collagen sponge (n=1 for each concentration). The control group received collagen only (Figure 2A, 2B) on the left side of mandible (n=3). The distance between the holes was 10 mm at the center of each hole. Two weeks later, beagles were sacrificed, and the bone was collected for the assessment of bone resorption around the holes.

Micro-CT analysis

The micro-CT machine and the conditions of micro-CT taking were described in 1.2. Alveolar bone regeneration in non-osteoporotic extraction sockets of the beagle dog maxilla. Bone volume (BV), tissue volume (TV), trabecular number (Tb.N), trabecular thickness (Tb.Th), trabecular spacing (Tb.Sp) and bone surface density (BSD) was analyzed for volumes of interest (VOIs) by CTAn 1.8 software program (Bruker micro CT, Kontich, Belgium). To determine the appropriate dose of RANKL to make a local osteoporotic model, the area around the hole (ø3 mm x 4 mm deep) that included 1 mm of the alveolar bone was designated as the VOI (ø5 mm x 4 mm height) which included 250 slices. Moreover, the values for the BV/TV, Tb.Th, Tb.N, Tb.Sp, and BMD for the 20-, 40-, and 60-μg RANKL treatments and collagen were only analyzed.

2.2. Evaluation of changes of bone quality at immediate after the RANKL removal, 4 and 6 weeks after the implant placement in the osteoporotic alveolar bone of the beagle dog mandible

Preparation of bone grafts to be applied at 4 and 6 weeks after the removal of RANKL

The compound (porous β-TCP microspheres and poloxamer hydrogel) was prepared as injectable β-TCP bone graft materials (ExcelOS Inject®, Bioalpha Inc., Seongnam, South Korea) (Figure 1B). In this experiment, as shown in Table 1, EXO-inject group received the compound-only and the other groups (BMP5, BMP15 and BMP45) received the compound containing 5, 15, and 45 μg of rhBMP-2 (from Escherichia coli, Bioalpha Inc., Seongnam, Korea), respectively. Different doses of rhBMP-2 were loaded into the compound by an in-situ mixing method.

Surgical procedure for implant placements at 4 and 6 weeks after the removal of RANKL

Seven one year old beagles, each weighing 12-13 kg, were used (n=7). The experimental protocol was approved by the institutional Animal Care and Use Committee, School of Dentistry, Seoul National University. All surgical procedures were aseptically performed with the animals under sedation with Zoletil 50 (0.05 mg/kg) and Rompun (0.15 mL/kg). Two months before RANKL application for creation of a localized osteoporotic mandible model, all mandibular premolars and first molars were extracted.

According to the results of the experimental set-up for a local osteoporotic model, the collagen absorbed 40 μg RANKL applied to the hole created a RANKL-induced local osteoporotic model. Two weeks later, secondary surgery was performed to remove the collagen sponge and to install the dental implant fixture with a diameter of 3.3 mm and depth of 6 mm (AnyRidge®, MegaGen Implant Co., Ltd., Gyeongsangbuk-do, Korea). For stable initial fixation of the dental implant, additional 2 mm deep holes were drilled with ø 2.8 mm in addition to the existing 4 mm deep holes (Figure 3A).

As shown in Table 1, the compound with various conditions (total of five groups) were injected and dental implants were installed on the holes. The Implant-only (no EXO-Inject) and the EXO-Inject only groups were placed on the right side, and the EXO-Inject groups, which included BMP5, BMP15 and BMP45, were placed on the left side. The distance between the groups was 10 mm at the center of each implant (Figure 3B). The alveolar crest was covered with collagen membranes over the cover screws of the implant to prevent penetration of gingival tissue between the implant and alveolar bone. Finally, the wound was closed with an absorbable suture material. Postoperative antibiotics and analgesics were administered for seven days. Animals were sacrificed four (n = 2) and six weeks (n = 5) after dental implant placement so that peri-implant bone generation could be determined. Implants including the

surrounding bone were sectioned for radiologic and histologic evaluations.

Micro-CT analysis

The micro-CT machine and the conditions of micro-CT taking were described in 1.2 Alveolar bone regeneration in non-osteoporotic extraction sockets of the beagle dog maxilla. The analysis parameters except BMD and software were described in 2.1 Evaluation of local osteoporosis induced by RANKL in the alveolar bone set-up model. Before BMD measurements, calibration procedures were performed with BMD calibration phantoms having known BMD values of 1.26 g/cm3 and 1.65 g/cm3, which consisted of fine calcium HA powder uniformly embedded in epoxy resin rods. BMDs were expressed in terms of grams per cubic centimeter of calcium HA in distilled water.

To evaluate the changes of bone quality on the mesial and distal side of holes and implants after the removal of RANKL, the BV/TV, Tb.Th, Tb.N, Tb.Sp, and BMD immediately after the removal of RANKL were evaluated in the local osteoporotic set-up model (Fig. 4A), and they were compared with the values at 4-weeks and 6-weeks after the removal of collagen sponges with RANKL in the implant placement models (Fig. 4B). The buccal and lingual side of the holes and implants were not included because of thin and various bone thickness. The size of VOI in A and B was 2.5 mm in buccolingual depth, 2 mm in

anteroposterior width and 4 mm in height from the alveolar crest in the local osteoporotic set-up model and from the upper margin of implant in the implant model. The inner border was distanced 1.65 mm from the center of the hole in the local osteoporotic set-up model (Fig. 4A) and from the center of the dental implant (3.3 mm in diameter) in the implant model (Fig. 4B).

3. Evaluation of peri-implant bone regeneration by injectable β-TCP bone grafts with different doses of rhBMP-2 on the osteoporotic alveolar bone of the beagle dog mandible at 4 and 6 weeks after implant placement

Micro-CT analysis

The micro-CT machine and the conditions of micro-CT taking were described in 1.2. Alveolar bone regeneration in non-osteoporotic extraction sockets of the beagle dog maxilla. The analysis software was described in 2.2. Evaluation of changes of bone quality at 2-, 4- and 6-weels after the removal of RANKL in the osteoporotic alveolar bone of the beagle dog mandible.

The β-TCP microspheres were not observed in the micro-CT images; therefore, they could not be distinguished or separated from the new bone on the micro-CT images in the

analysis because they consisted of tiny particles and were almost absorbed. Additionally, a small amount of unabsorbed particles was observed only in the histological slide (Figure 5B, 5C).

To evaluate peri-implant alveolar bone regeneration, each VOI (5 mm in diameter) consisted of three inter-thread space from the second to fifth thread (350 slices, approximately3 mm in height) was determined, and BV / TV, Tb.Th, Tb.N, Tb.Sp, and BMD were calculated (Figure 4C).

Histologic analysis

After micro-CT images were obtained, the blocks of undecalcified specimens were sectioned through the middle of implant parallel to the long axis of the implant. These specimens were dehydrated in alcohol rinses and embedded in an Osteo-Bed resin (Technovit 7210, Kulzer, Wehrheim, Germany). Blocks of polymerized specimens with implants cut to a final thickness of 50 μm using an EXAKT grinding machine (BS-3000N, EXAKT, Norderstedt, Germany), and two sections per bone tissue block were acquired. One section was stained with hematoxylin and eosin (H&E), and the other section was stained with Masson's trichrome (MT). Digital images of the stained sections were captured with an Olympus BX51 transmission and polarized optical microscope Axioskop (Olympus Corporation, Tokyo, Japan) equipped with a digital camera (SPOT Insight, Diagnostic Instrument, Inc., Sterling

Heights, MI, USA). To evaluate the peri-implant bone formation, the new bone area and the total area within the inter-thread area from the second to the fifth thread crest on both sides of the implant (Fig. 5A) were measured with the Image J software (National Institutes of Health, Bethesda, MD, USA), and the bone area (%) was calculated from the ratio of the new bone area to the total area. For the BIC measurements, the total length and the bone contact length along the implant surface from the second to fifth thread crest on both sides of the implant were measured with the SPOT software (Diagnostic Instruments, Inc., Sterling Height, MI, USA).

4. Statistical analysis

All data are presented as mean ± standard error of the mean or standard deviation. Statistical analyses were performed with SPSS statistical software version 23 (IBM, Armonk, NY, USA). Data between the two groups were compared by a Mann-Whitney U test, and the comparison of data in more than two groups was done by Kruskal-Wallis test. Differences with $p<0.05$ were considered significant.

Ⅲ. Results

1. rhBMP-2 release profiles by injectable β-TCP microspheres

The β-TCP microspheres showed significantly more sustained release during first 12 hours ($p < 0.05$), and it was significantly much slower after 12 hours ($p < 0.001$ at 1d, 2d, 5d, 12d, 19d and 26d), and the amount of rhBMP-2 released after 26 days was less than 21 % of the total dose (Figure 6). The β-TCP microspheres also showed a more sustained release compared to TCP ($p<0.05$ at 1d, 2d, 5d, 12d, 19d and 26d), HA ($p<0.05$ at 2d, 5d, 12d, 19d and 26d), and biphasic calcium phosphate granules ($p<0.05$ at 5d, 12d, 19d and 26d) (Figure 6).

2. Effect of injectable β-TCP bone grafts combined with rhBMP-2 on alveolar bone regeneration in non-osteoporotic extraction sockets of the beagle dog maxilla

Micro-CT analysis

Both the control and experimental groups clearly showed new bone formation, and injectable β-TCP microspheres penetrated into the spaces of the surrounding trabecular bone (Figure 7). The extraction socket walls remained in both the groups. However, BV (mm^{3}), BV / TV (%) and Tb.N (1/mm)

values were significantly higher in the experimental group than those in the control group ($p<0.05$) (Table 2).

Histologic analysis

In both the groups, new bone formation without any inflammation was observed (Figure 8). BA (%) in the experimental group (54%) was higher than that in the control group (49%), but the difference was not significant. Some β-TCP microspheres were not absorbed in the center of the extraction sockets in both the groups. In the experimental group, unabsorbed β-TCP microspheres were completely embedded in the newly formed trabecular bone, whereas in the control group, some unabsorbed β-TCP microspheres did not surround the new bone (Figure 8)

3. Local osteoporosis induced by RANKL in the alveolar bone set-up model

Bone resorption appeared at over 40 μg of RANKL. Compared with the control group, BV was reduced by 41.60% and 45.62% at 40 and 60 μg of RANKL, respectively (Figure 9A) (Table. 3). However, there was a slightly increase in BV at 20 μg of RANKL. With RANKL at 60 μg, the absorbed bone mass was similar to that of the 40 μg RANKL treated group, and the concentration for inducing osteoporosis was determined as 40 μg RANKL. Clinically, an inflammatory reaction of the gums was

observed in the experimental group (Figure 9B). It was confirmed that sufficient osteoporosis was generated by the application of RANKL for two weeks.

4. Changes of bone quality at immediate after the RANKL removal, 4 and 6 weeks after implant placement in the osteoporotic alveolar bone of the beagle dog mandible

Comparison of the bone quality between the control and the RANKL-applied group immediately after the removal of RANKL

Immediately after the removal of RANKL, there were no significant differences in the micro-CT values between the RANKL applied group and the control group on the mesial and distal side of defect holes (Table 4).

Changes of bone quality at the outside of defect holes/inter-thread space from immediately after the RANKL removal, 4 and 6 weeks after the implant placement

When only the Implant group was evaluated, the bone quality on the mesial and distal side of inter-thread space was partly (BV/TV, Tb.Th) reduced at 4 weeks after implant placement, compared to it immediately after the removal of RANKL (no statistical analysis due to the small sample number in the 4 weeks group). However, the BV/TV, Tb.N and BMD were significantly increased at 6 weeks compared to them immediately after the removal of RANKL ($p < 0.05$) (Table 5).

When all cases in the same waiting period were classified into a same group, independent of the use of injectable graft material and the concentration of rhBMP-2, the BV/TV (51.91%) and BMD (1.45 mg/cc) at 6 weeks were highly increased than them at 4 weeks (30.64%, 1.36 mg/cc, respectively) ($p < 0.001$), which were slight lower to them immediately after the removal of RANKL (32.85%, 1.37 mg/cc, respectively) (Table 6, Figure 10).

Comparison of the bone regeneration within inter-thread space between the 4 weeks and the 6 weeks groups

In terms of the inter-thread space, when only the Implant group was evaluated, the bone regeneration at 6 weeks was increased in the values of micro-CT (BV/TV, Tb.Th, BMD) and in the histomorphometric values (BA and BIC), compared to it at 4 weeks (no statistical analysis due to the small sample number in the 4-weeks group) (Table 7). When all cases in the same waiting period were classified into a same group, independent on the use of injectable graft material and the concentration of rhBMP-2, all values at 6 weeks were significantly greater than them at 4 weeks. The BV/TV (12.73%) and BMD (1.27 mg/cc), the BA (40.17%) at 4 weeks were increased to 15.10% and 1.31 mg/cc and 53.03%, respectively at 6 weeks ($p < 0.001$) (Table 8).

5. Peri-implant bone regeneration by injectable β-

TCP bone grafts with different doses of rhBMP-2 on the osteoporotic alveolar bone of the beagle dog mandible at 4 and 6 weeks after implant placement

Micro-CT analysis

The BV/TV values in the EXO-Inject group and BMP5 group were higher than other groups at 4 weeks after implant placement. However, no statistical significant in all groups, due to the small number of case (n=2) at the 4 weeks. (Table 10) The BV/TV in the BMP5 group (27.22 %) was the highest among the groups and statistically greater compared with that in the implant-only group (23.14%) and the BMP45 group (22.97%) ($p<0.05$) at six weeks after implant placement (Table 11). The BV/TV in the EXO-inject group (26.23%) was statistically higher than that in the Implant only group (23.14%). The BV/TV in the BMP5 group was higher than that in the EXO-inject group; however, the difference was not significant. The BV/TV in the BMP15 and BMP45 groups was lower than even that in the implant-only group. The BMP45 group had a significantly higher value for Tb.Th. than that in the implant-only group. The BMD was significantly higher in the BMP5 group than in the Implant only group (Table 11, Figure 11)

Histologic analysis

Undecalcified histologic slides were prepared, H&E staining was performed, and bone formation around the implant threads was observed. Through MT staining of the RANKL treatment

site, it could clearly be observed how new bone formed at the site of bone resorption. When the dental implants were installed after application of the injectable β-TCP bone grafts with or without BMP, the new bone was seen to flow into the implant thread surfaces and to adhere well to the implant surface. In the EXO-inject and BMP5 group, newly formed bone was evident around the fixture and fused with the fixture in 4 weeks and 6 weeks. However, in the BMP15 and BMP45, the amount of new bone around the dental implant was clearly smaller compared with that in the other groups (Figure 12). The BA (%) and BIC (%) values were the highest in the BMP5 (43.80 %, 50.34%, respectively) group compared to other groups at 4 weeks. However, there was no statistical significance due to the small number of case at 4 weeks (Table 12). However, the BA (%) and BIC (%) values were significantly higher in the EXO-Inject (51.97%, 58.10%, respectively) and BMP5 (58.49%, 66.56%, respectively) groups compared to the Implant only group (44.05%, 50.05%, respectively) at 6 weeks ($p<0.05$) (Table 13). While there was no significant difference in the BA between the two groups, the BMP5 group (66.56%) had a significantly higher BIC than that of the EXO-Inject (58.10%) ($p<0.05$) and BMP45 ($p<0.001$) (52.44%) groups. As the BMP-2 concentration increased in the injectable bone grafts, the BA and BIC values tended to decrease (Table 13, Figure 13)

Ⅳ. DISCUSSION

We evaluated the release kinetics of rhBMP-2 from β-TCP microspheres and the effect of injectable β-TCP microsphere bone grafts with rhBMP-2 in non-osteoporotic extraction sockets and newly developed osteoporotic alveolar bone model of beagle dogs. A more sustained release of rhBMP-2 was observed from injectable β-TCP microspheres than from other carrier types such as collagen sponge, granule HAs, β-TCP, and biphasic calcium phosphates (Figure 6). The local osteoporotic alveolar bone model of beagle dogs was developed using collagen sponges soaked with 40 μg RANKL, which were applied into holes in the alveolar bone for two weeks (Figure 2, Table 3). Then, the consequent changes of bone quality at immediately after RANKL removal and four and six weeks after implant placement were investigated. As a result, there was no significant differences in the bone volume fraction (BV/TV) and the BMD between immediately after RANKL removal (32.85%, 1.37 mg/cc) and 4 weeks after implant placement (30.64%, 1.36 mg/cc), but that value was significantly increased at 6 weeks (51.91%, 1.45 mg/cc) compared to 4 weeks after implant placement (Table 6, Figure 10) ($p<0.001$). Therefore, we found that bone regeneration was activated between 4 weeks and 6 weeks after implant placement (Table 6). However, when the BV/TV increase rate between inside and outside of the inter-thread area were

compared at 4 weeks and 6 weeks after implant placement, that of the inside area (20.36%) was statistically significantly lower than that of the outside area (73.97%) in all groups ($p<0.05$) (Table 6, 8, 9). Therefore, we assumed that RANKL still remained active within the inter-thread area at 6 weeks after implant placement. Finally, the new injectable β-TCP microsphere bone grafts could be effectively evaluated with increasing bone formation around the implants at 4 weeks and 6 weeks after implant placement, particularly in injectable β-TCP microsphere bone grafts containing 5 μg of BMP-2. However, the bone formation efficacy was not enhanced with increasing BMP-2 concentrations (Table 10-13, Figure 11-13).

Although rhBMP-2 has been shown to have strong osteoinductive activity (146-148), its use in humans have not been sufficiently clear (28,75,79) and its higher doses are required to obtain a significant bone regeneration effect (27, 75, 79). One of the reasons for the unclear results in human clinical applications has been attributed to the unfavorable release of the rhBMP-2 due to inherent characteristics of carriers. Therefore, for the sustained release of rhBMP-2, various carrier materials, including diverse hydrogels (8, 147, 151, 152), collagen sponges combined with heparin (150), and bisphosphonates (148, 149, 153, 154) have been introduced. Compared with a collagen sponge alone (155), rhBMP-2 has a

more sustained release from the collagen sponge coated with HA. The amount of rhBMP-2 released from the collagen sponge coated with HA was 45–50% of that released from the collagen sponge alone (148). A test for assessing rhBMP-2 retention and new bone induction with HA and β-TCP, which were placed in the subcutis of rats, revealed that the amount of BMP-2 remaining in β-TCP was 49.6% at 1 day and 32.5% at 3 weeks after implantation and that the amount of BMP-2 remaining in HA was 34.0% at 1 day and 3.0% at 3 weeks (32). Based on those studies, we can infer that a more sustained release of rhBMP-2 is observed from β-TCP than from collagen sponge or HA. Moreover, the total surface area of β-TCP microspheres is larger than that of granule β-TCPs, and the loaded amount of rhBMP-2 could be increased, probably because of the enhanced growth factor retention. In this study, a more sustained release was observed from β-TCP microspheres than from granule β-TCPs, despite their similar chemistry ($p < 0.05$ at 1, 2, 5, 12, 19, and 26 days; Figure 6). This suggests that the affinity and release kinetics of rhBMP-2 to calcium phosphates is enhanced as the area of binding site increases.

The new injectable bone graft material used in this study confirmed the bone formation effect around the implant. This bone graft material mainly comprises porous β-TCP microspheres (particle size, 45–75 μm) and poloxamer

hydrogel, it can be easily injected, and it has better penetration into narrow spaces and better reduction of spaces between implant surfaces and bone grafts than the granule-type bone graft material (particle size, 0.6–2.0 mm). This feature may be helpful for bone formation (145) in patients with osteoporosis because the new bone graft material can fill the spaces in cases wherein Tb.N is decreased and Tb.Sp is increased, both of which are characteristic features of osteoporosis. Compared with the implant-only group, we found that the BV/TV value in the micro-CT analysis and the BA and BIC values in the histologic analysis were significantly increased in the EXO-inject group ($p<0.05$). These data demonstrate the potential good bone-forming effects of β-TCP microspheres without growth factors in an osteoporotic environment.

We established a new local osteoporotic alveolar bone of the beagle dog mandible using local RANKL application. Micro-CT analysis showed the bone volume fraction (BV/TV) was significantly reduced after two weeks of RANKL application (40 and 60 μg/collagen) to beagle mandibles (Figure 9A, Table 3). We used 40μg RANKL/collagen because it resulted in a bone volume (BV) reduction comparable to that obtained with 60μg RANKL/collagen. This established an osteoporotic model with several advantages. First, the model could be created rapidly in two weeks. Previous studies have shown that bone composition in dogs is the most similar to that in humans and is suitable for

studying bone metabolism disease. However, osteoporosis induction is difficult and takes 8-12 months after ovariectomy for it to be observed (39, 40, 42, 82). Second, the model can easily be created using RANKL application to the experimental site, without the the technical skills required for an ovariectomy. Bone volume can be easily decreased with an increasing dose of RANKL, while low-dose RANKL promotes bone formation (54). In addition, the mechanism of bone loss is simple. High-dose RANKL directly mediates osteoclast activation and differentiation. In our local osteoporotic model using RANKL, the rapid reduction of BV was apparently caused by the stimulation of the final differentiation of osteoclast progenitors and existing osteoclasts. To observe an effect on bone loss due to systemic injections of RANKL, RANKL should be injected every 24 hours for two days to two weeks, because the osteoclast activity in response to exogenously injected RANKL differs from the normal activity of osteoclasts affected by osteoblast membrane-bound RANKL (56, 141). Therefore, a local application of RANKL may be beneficial because a single surgery at the local experimental site can easily lead to bone resorption. It is important to induce osteoporosis directly at the testing site, because the other parts of the body may not be affected even though osteoporosis may be diagnosed in some parts of the skeleton (7).

It should be noted that the RANKL-induced local

osteoporotic alveolar bone in the beagle dog mandible model may not completely reproduce the osteoporosis phenomenon caused by hormonal changes after menopause or aging. However, according to the Lekholm and Zarb classification (142), osteoporotic bone is similar to that in the type IV bone model, which has a thin layer of cortical bone and low-density trabecular bone. In our locally developed osteoporotic model with 40, 60 μg/collagen, a low value of trabecular bone volume, trabecular thickness, and trabecular number were observed. It has been shown that was osteoprotegerin production is reduced due to low levels of serum estrogen in patients who developed osteoporosis after menopause (143, 144), and that a relatively RANKL-active environment was created. Unlike osteoporosis occurring due to hormonal deficiency, local osteoporosis induced by a single application of RANKL can only continue for a limited time. Because further applications of RANKL to the specific bone space during ongoing tests are difficult or impossible in most cases, an optimal dose and application duration should be well established for each purpose. Another challenge of using RANKL-induced local osteoporosis is that RANKL stimulates new bone formation. In our set-up experiment for the local osteoporotic alveolar bone of the beagle dog mandible, the application of 20 μg of RANKL increased the BV/TV, which is consistent with the finding that a low-dose of RANKL promotes bone formation (54). Moreover, new bone within the marrow space was strongly

increased during the time interval between four and six weeks after the implant placement. Therefore, it seems that the osteoporotic status induced by RANKL can be maintained only for four weeks. The RANKL-induced local osteoporosis model can be used to evaluate new bone substitutes and new implant designs and surfaces in patients with catabolic bone metabolism, however only for the early stage within four weeks. When RANKL is applied locally, the duration of the RANKL effect and the surrounding tissue penetration ratio may be different depending on the bone metabolic status even in similarly aged individuals. Further studies with a large number of animals are needed to elucidate the mechanism of the delayed osteogenesis using high dose of RANKL.

The establishment of an effective rhBMP-2 dose to induce enhanced osteogenesis is important, because it would be different in the anabolic or catabolic bone status. In non-osteoporotic maxillary first molar extraction sockets of beagle dogs, β-TCP microsphere bone grafts with 45ug rhBMP-2 showed higher bone forming effect ($p<0.05$) (Table 2). However, in the RANKL-induced osteoporotic alveolar bone, the bone forming effect was the highest in the group wherein 5μg rhBMP-2 was added, and the effect of bone formation was reduced with increasing rhBMP-2 concentration. It is well known that BMP-2 can not only stimulate the differentiation of stem cells and preosteoblasts into osteoblasts, but also the

activation of osteoclasts (11, 156, 157), particularly at high doses (11), thus leading to bone resorption. In a sheep model, Toth et al. (2009) reported that increasing local BMP-2 levels led to enhanced osteoclastic resorption of the peri-implant bone (74). However, this osteoclastic effect was transient and followed by progressive bone healing and formation (143, 144, 146). The current literature suggests that BMP-2 activates osteoclasts directly through Smad signaling (22, 77), and indirectly through osteoclastic-promoting factors including RANKL produced by osteoblasts (78). The enhanced expression of osteoclast differentiation genes by BMP-2 was dependent on RANKL. In the absence of RANKL, BMP-2 was unable to induce osteoclast differentiation (77). These findings support those of Itoh et al. (2001) suggesting that BMP-2 induced enhancement of osteoclast differentiation was caused by cross-communication between BMP receptor-mediated signals and RANK-mediated signals (76). In the present study with the osteoporotic status induced by RANKL application for two weeks, a high concentration of rhBMP-2 could indirectly or directly activate more osteoclasts through RANKL-mediated or RANKL-dependent osteoclastogenesis pathway. Therefore, it seems that the bone formation effect in the BMP15 and BMP45 groups was less than that in the BMP5 group (Table 10-13, Figure 11-13), and a low dose of rhBMP-2 is recommended in the osteoporotic alveolar bone induced by RANKL.

Ⅴ. CONCLUSIONS

The new injectable bone graft comprising porous β-TCP microspheres and poloxamer hydrogels possesses the sustained-release property of rhBMP-2, convenient loading property of rhBMP-2 using the in situ mixing method, and easy handling for transplantation, which can enhance bone regeneration.

A newly developed local osteoporotic alveolar bone model of beagle dogs was developed using collagen sponges soaked with 40μg RANKL, which were applied into holes in the alveolar bone for two weeks. In our RANKL-induced osteoporotic alveolar bone, the initial bone quality outside the inter-thread space was slightly decreased at four weeks after the removal of RANKL, while it was actively increased at six weeks. The bone quality within the inter-thread space at four weeks was comparable with that immediately after the removal of RANKL, and it was significantly higher at six weeks than it was at four weeks. The local osteoporotic status in the alveolar bone induced by 40μg RANKL can apparently persist until four weeks after the removal of RANKL.

Finally, the new injectable β-TCP bone grafts could be effectively evaluated with increasing bone formation around the implants, particularly in injectable β-TCP bone grafts containing 5μg rhBMP-2. However, the bone formation efficacy

was not enhanced with increasing BMP-2 concentrations. Our local osteoporotic beagle dog mandible model could be useful to evaluate new bone graft materials and implant surfaces to improve bone formation in geriatric patients with osteoporosis.

Ⅵ. References

1. Becker W, Hujoel PP, Becker BE, Willingham H. Osteoporosis and implant failure: an exploratory case-control study. J Periodontol. 2000;71(4):625-31.

2. Lugero GG, de Falco Caparbo V, Guzzo ML, Konig B, Jr., Jorgetti V. Histomorphometric evaluation of titanium implants in osteoporotic rabbits. Implant Dent. 2000;9(4):303-9.

3. Cho P, Schneider GB, Krizan K, Keller JC. Examination of the bone-implant interface in experimentally induced osteoporotic bone. Implant Dent. 2004;13(1):79-87.

4. Narai S, Nagahata S. Effects of alendronate on the removal torque of implants in rats with induced osteoporosis. Int J Oral Maxillofac Implants. 2003;18(2):218-23.

5. Fini M, Giavaresi G, Rimondini L, Giardino R. Titanium alloy osseointegration in cancellous and cortical bone of ovariectomized animals: histomorphometric and bone hardness measurements. Int J Oral Maxillofac Implants. 2002;17(1):28-37.

6. Qi M, Hu J, Li J, Li J, Dong W, Feng X, et al. Effect of zoledronate acid treatment on osseointegration and fixation of implants in autologous iliac bone grafts in ovariectomized rabbits. Bone. 2012;50(1):119-27.

7. Dao TT, Anderson JD, Zarb GA. Is osteoporosis a risk factor for osseointegration of dental implants? Int J Oral Maxillofac Implants. 1993;8(2):137-44.

8. Pan H, Han JJ, Park Y-D, Cho TH, Hwang SJ. Effect of sustained release of rhBMP-2 from dried and wet hyaluronic acid hydrogel carriers compared with direct dip coating of rhBMP-2 on peri-implant osteogenesis of dental implants in canine mandibles. Journal of Cranio-Maxillofacial Surgery. 2016;44(2):116-25.

9. Wikesjö UM, Qahash M, Polimeni G, Susin C, Shanaman RH, Rohrer MD, et al. Alveolar ridge augmentation using implants coated with recombinant human bone morphogenetic protein-2: histologic observations. Journal of clinical periodontology. 2008;35(11):1001-10.

10. Hanisch O, Tatakis DN, Boskovic MM, Rohrer MD, Wikesjö UM. Bone formation and reosseointegration in peri-implantitis defects following surgical implantation of rhBMP-2. International Journal of Oral & Maxillofacial Implants. 1997;12(5).

11. Seeherman HJ, Li XJ, Bouxsein ML, Wozney JM. rhBMP-2 induces transient bone resorption followed by bone formation in a nonhuman primate core-defect model. The Journal of Bone & Joint Surgery. 2010;92(2):411-26.
12. Sharma A, Meyer F, Hyvonen M, Best S, Cameron R, Rushton N. Osteoinduction by combining bone morphogenetic protein (BMP)-2 with a bioactive novel nanocomposite. Bone and Joint Research. 2012;1(7):145-51.
13. Sampath TK, Maliakal J, Hauschka P, Jones W, Sasak H, Tucker R, et al. Recombinant human osteogenic protein-1 (hOP-1) induces new bone formation in vivo with a specific activity comparable with natural bovine osteogenic protein and stimulates osteoblast proliferation and differentiation in vitro. Journal of Biological Chemistry. 1992;267(28):20352-62.
14. Urist MR. Bone: formation by autoinduction. Science. 1965;150(3698):893-9.
15. Wildemann B, Burkhardt N, Luebberstedt M, Vordemvenne T, Schmidmaier G. Proliferating and differentiating effects of three different growth factors on pluripotent mesenchymal cells and osteoblast like cells. Journal of orthopaedic surgery and research. 2007;2(1):27.
16. Haidar ZS, Hamdy RC, Tabrizian M. Delivery of recombinant bone morphogenetic proteins for bone regeneration and repair. Part A: current challenges in BMP delivery. Biotechnology letters. 2009;31(12):1817.
17. Haidar ZS, Hamdy RC, Tabrizian M. Delivery of recombinant bone morphogenetic proteins for bone regeneration and repair. Part B: Delivery systems for BMPs in orthopaedic and craniofacial tissue engineering. Biotechnology letters. 2009;31(12):1825-35.
18. Carragee EJ, Hurwitz EL, Weiner BK. A critical review of recombinant human bone morphogenetic protein-2 trials in spinal surgery: emerging safety concerns and lessons learned. The Spine Journal. 2011;11(6):471-91.
19. Zara JN, Siu RK, Zhang X, Shen J, Ngo R, Lee M, et al. High doses of bone morphogenetic protein 2 induce structurally abnormal bone and inflammation in vivo. Tissue Engineering Part A. 2011;17(9-10):1389-99.
20. Burkus JK, Gornet MF, Dickman CA, Zdeblick TA. Anterior lumbar interbody fusion using rhBMP-2 with tapered interbody cages. Clinical Spine Surgery. 2002;15(5):337-49.
21. Burkus JK, Sandhu HS, Gornet MF. Influence of rhBMP-2 on the healing patterns associated with allograft interbody constructs in comparison with

autograft. Spine. 2006;31(7):775-81.
22. Kaneko H, Arakawa T, Mano H, Kaneda T, Ogasawara A, Nakagawa M, et al. Direct stimulation of osteoclastic bone resorption by bone morphogenetic protein (BMP)-2 and expression of BMP receptors in mature osteoclasts. Bone. 2000;27(4):479-86.
23. Smucker JD, Rhee JM, Singh K, Yoon ST, Heller JG. Increased swelling complications associated with off-label usage of rhBMP-2 in the anterior cervical spine. Spine. 2006;31(24):2813-9.
24. Epstein NE. Basic science and spine literature document bone morphogenetic protein increases cancer risk. Surgical neurology international. 2014;5(Suppl 15):S552.
25. Winn SR, Uludag H, Hollinger JO. Carrier systems for bone morphogenetic proteins. Clinical orthopaedics and related research. 1999;367:S95-S106.
26. Uludag H, D'Augusta D, Palmer R, Timony G, Wozney J. Characterization of rhBMP-2 pharmacokinetics implanted with biomaterial carriers in the rat ectopic model. Journal of Biomedical Materials Research Part A. 1999;46(2):193-202.
27. Fiorellini JP, Howell TH, Cochran D, Malmquist J, Lilly LC, Spagnoli D, et al. Randomized study evaluating recombinant human bone morphogenetic protein-2 for extraction socket augmentation. Journal of periodontology. 2005;76(4):605-13.
28. Kim Y-J, Lee J-Y, Kim J-E, Park J-C, Shin S-W, Cho K-S. Ridge preservation using demineralized bone matrix gel with recombinant human bone morphogenetic protein-2 after tooth extraction: a randomized controlled clinical trial. Journal of Oral and Maxillofacial Surgery. 2014;72(7):1281-90.
29. Huh J-B, Lee H-J, Jang J-W, Kim M-J, Yun P-Y, Kim S-H, et al. Randomized clinical trial on the efficacy of Escherichia coli-derived rhBMP-2 with β-TCP/HA in extraction socket. The journal of advanced prosthodontics. 2011;3(3):161-5.
30. Bohner M. Calcium orthophosphates in medicine: from ceramics to calcium phosphate cements. Injury. 2000;31:D37-D47.
31. Luca L, Rougemont AL, Walpoth BH, Boure L, Tami A, Anderson JM, et al. Injectable rhBMP-2-loaded chitosan hydrogel composite: Osteoinduction at ectopic site and in segmental long bone defect. Journal of biomedical materials research Part A. 2011;96(1):66-74.

32. Tazaki J, Murata M, Akazawa T, Yamamoto M, Ito K, Arisue M, et al. BMP-2 release and dose-response studies in hydroxyapatite and β-tricalcium phosphate. Bio-medical materials and engineering. 2009;19(2-3):141-6.
33. Lee JH, Baek H-R, Lee KM, Lee H-K, Im SB, Kim YS, et al. The Effect of Poloxamer 407-Based Hydrogel on the Osteoinductivity of Demineralized Bone Matrix. Clinics in orthopedic surgery. 2014;6(4):455-61.
34. Lee JH, Ryu MY, Baek HR, Lee HK, Seo JH, Lee KM, et al. The Effects of Recombinant Human Bone Morphogenetic Protein-2-Loaded Tricalcium Phosphate Microsphere–Hydrogel Composite on the Osseointegration of Dental Implants in Minipigs. Artificial organs. 2014;38(2):149-58.
35. Kim RY, Oh JH, Lee BS, Seo Y-K, Hwang SJ, Kim IS. The effect of dose on rhBMP-2 signaling, delivered via collagen sponge, on osteoclast activation and in vivo bone resorption. Biomaterials. 2014;35(6):1869-81.
36. Kim SK, Cho TH, Han JJ, Kim IS, Park Y, Hwang SJ. Comparative study of BMP-2 alone and combined with VEGF carried by hydrogel for maxillary alveolar bone regeneration. Tissue Engineering and Regenerative Medicine. 2016;13(2):171-81.
37. Dumortier G, Grossiord JL, Agnely F, Chaumeil JC. A review of poloxamer 407 pharmaceutical and pharmacological characteristics. Pharmaceutical research. 2006;23(12):2709-28.
38. Yu CH, Lee JH, Baek H-R, Nam H. The effectiveness of poloxamer 407-based new anti-adhesive material in a laminectomy model in rats. European Spine Journal. 2012;21(5):971-9.
39. Pearce AI, Richards RG, Milz S, Schneider E, Pearce SG. Animal models for implant biomaterial research in bone: a review. Eur Cell Mater. 2007;13:1-10.
40. Turner AS. Animal models of osteoporosis--necessity and limitations. Eur Cell Mater. 2001;1:66-81.
41. Aerssens J, Boonen S, Lowet G, Dequeker J. Interspecies differences in bone composition, density, and quality: potential implications for in vivo bone research. Endocrinology. 1998;139(2):663-70.
42. Shen V, Dempster DW, Birchman R, Mellish RW, Church E, Kohn D, et al. Lack of changes in histomorphometric, bone mass, and biochemical parameters in ovariohysterectomized dogs. Bone. 1992;13(4):311-6.
43. Faugere MC, Friedler RM, Fanti P, Malluche HH. Bone changes occurring early after cessation of ovarian function in beagle dogs: a histomorphometric

study employing sequential biopsies. J Bone Miner Res. 1990;5(3):263-72.
44. Boyce RW, Franks AF, Jankowsky ML, Orcutt CM, Piacquadio AM, White JM, et al. Sequential histomorphometric changes in cancellous bone from ovariohysterectomized dogs. J Bone Miner Res. 1990;5(9):947-53.
45. Drezner MK, Nesbitt T. Role of calcitriol in prevention of osteoporosis: Part I. Metabolism. 1990;39(4):18-23.
46. Tsutsumi R, Xie C, Wei X, Zhang M, Zhang X, Flick LM, et al. PGE2 signaling through the EP4 receptor on fibroblasts upregulates RANKL and stimulates osteolysis. Journal of Bone and Mineral Research. 2009;24(10):1753-62.
47. Kong Y-Y, Feige U, Sarosi I, Bolon B, Tafuri A, Morony S, et al. Activated T cells regulate bone loss and joint destruction in adjuvant arthritis through osteoprotegerin ligand. Nature. 1999;402:43-7.
48. Kim N, Odgren PR, Kim D-K, Marks SC, Choi Y. Diverse roles of the tumor necrosis factor family member TRANCE in skeletal physiology revealed by TRANCE deficiency and partial rescue by a lymphocyte-expressed TRANCE transgene. Proceedings of the National Academy of Sciences. 2000;97(20):10905-10.
49. Dougall WC, Glaccum M, Charrier K, Rohrbach K, Brasel K, De Smedt T, et al. RANK is essential for osteoclast and lymph node development. Genes & development. 1999;13(18):2412-24.
50. Li J, Sarosi I, Yan X-Q, Morony S, Capparelli C, Tan H-L, et al. RANK is the intrinsic hematopoietic cell surface receptor that controls osteoclastogenesis and regulation of bone mass and calcium metabolism. Proceedings of the National Academy of Sciences. 2000;97(4):1566-71.
51. Kong Y-Y, Yoshida H, Sarosi I, Tan H-L, Timms E, Capparelli C, et al. OPGL is a key regulator of osteoclastogenesis, lymphocyte development and lymph-node organogenesis. Nature. 1999;397(6717):315-23.
52. Mizuno A, Amizuka N, Irie K, Murakami A, Fujise N, Kanno T, et al. Severe osteoporosis in mice lacking osteoclastogenesis inhibitory factor/osteoprotegerin. Biochemical and biophysical research communications. 1998;247(3):610-5.
53. Bucay N, Sarosi I, Dunstan CR, Morony S, Tarpley J, Capparelli C, et al. Osteoprotegerin-deficient mice develop early onset osteoporosis and arterial calcification. Genes & development. 1998;12(9):1260-8.
54. Cline-Smith A, Gibbs J, Shashkova E, Buchwald ZS, Novack DV, Aurora R. Pulsed low-dose RANKL as a potential therapeutic for postmenopausal osteoporosis. JCI insight. 2016;1(13).

55. Cummings SR, Martin JS, McClung MR, Siris ES, Eastell R, Reid IR, et al. Denosumab for prevention of fractures in postmenopausal women with osteoporosis. New England Journal of Medicine. 2009;361(8):756-65.
56. Tomimori Y, Mori K, Koide M, Nakamichi Y, Ninomiya T, Udagawa N, et al. Evaluation of pharmaceuticals with a novel 50-hour animal model of bone loss. Journal of Bone and Mineral Research. 2009;24(7):1194-205.
57. Li J, Zeng L, Xie J, Yue Z, Deng H, Ma X, et al. Inhibition of Osteoclastogenesis and Bone Resorption in vitro and in vivo by a prenylflavonoid xanthohumol from hops. Scientific reports. 2015;5.
58. Chang E-J, Kim HJ, Ha J, Kim HJ, Ryu J, Park K-H, et al. Hyaluronan inhibits osteoclast differentiation via Toll-like receptor 4. Journal of cell science. 2007;120(1):166-76.
59. Reddi AH. Bone Morphogenetic Proteins, Bone Marrow Stromal Cells, and Mesenchymal Stem Cells: Maureen Owen Revisited. Clinical orthopaedics and related research. 1995;313:115-9.
60. Wozney JM, Rosen V, Celeste AJ, Mitsock LM, Whitters MJ, Kriz RW, et al. Novel regulators of bone formation: molecular clones and activities. Science. 1988;242(4885):1528-35.
61. Groeneveld E, Burger E. Bone morphogenetic proteins in human bone regeneration. European journal of endocrinology. 2000;142(1):9-21.
62. Cunningham NS, Jenkins NA, Gilbert DJ, Copeland NG, Reddi AH, Lee S-J. Growth/differentiation factor-10: A new member of the transforming growth factor-β superfamily related to bone morphogenetic protein-3. Growth Factors. 1995;12(2):99-109.
63. Mayer H, Scutt A, Ankenbauer T. Subtle differences in the mitogenic effects of recombinant human bone morphogenetic proteins− 2 to− 7 on DNA synthesis on primary bone-forming cells and identification of BMP-2/4 receptor. Calcified tissue international. 1996;58(4):249-55.
64. Boden SD, McCuaig K, Hair G, Racine M, Titus L, Wozney JM, et al. Differential effects and glucocorticoid potentiation of bone morphogenetic protein action during rat osteoblast differentiation in vitro. Endocrinology. 1996;137(8):3401-7.
65. Haÿ E, Marie P, Debiais F. Regulation of human cranial osteoblast phenotype by FGF-2, FGFR-2 and BMP-2 signaling. Histology and histopathology. 2002.

66. Burkus JK, Transfeldt EE, Kitchel SH, Watkins RG, Balderston RA. Clinical and radiographic outcomes of anterior lumbar interbody fusion using recombinant human bone morphogenetic protein-2. Spine. 2002;27(21):2396-408.
67. Rengachary SS. Bone morphogenetic proteins: basic concepts. Neurosurgical focus. 2002;13(6):1-6.
68. Shi Y, Massagué J. Mechanisms of TGF-β signaling from cell membrane to the nucleus. Cell. 2003;113(6):685-700.
69. ten Dijke P, Korchynskyi O, Valdimarsdottir G, Goumans M-J. Controlling cell fate by bone morphogenetic protein receptors. Molecular and cellular endocrinology. 2003;211(1):105-13.
70. Jason JY, Barnes AP, Hand R, Polleux F, Ehlers MD. TGF-β signaling specifies axons during brain development. Cell. 2010;142(1):144-57.
71. Jeon MJ, Kim JA, Kwon SH, Kim SW, Park KS, Park S-W, et al. Activation of peroxisome proliferator-activated receptor-γ inhibits the Runx2-mediated transcription of osteocalcin in osteoblasts. Journal of Biological Chemistry. 2003;278(26):23270-7.
72. Liu J, Chen L, Liu X, Tang K. Insulin-like growth factor-1 and bone morphogenetic protein-2 jointly mediate prostaglandin E2-induced adipogenic differentiation of rat tendon stem cells. PloS one. 2014;9(1):e85469.
73. Suda T, Takahashi N, Udagawa N, Jimi E, Gillespie MT, Martin TJ. Modulation of osteoclast differentiation and function by the new members of the tumor necrosis factor receptor and ligand families. Endocrine reviews. 1999;20(3):345-57.
74. Toth JM, Boden SD, Burkus JK, Badura JM, Peckham SM, McKay WF. Short-term osteoclastic activity induced by locally high concentrations of recombinant human bone morphogenetic protein–2 in a cancellous bone environment. Spine. 2009;34(6):539-50.
75. James AW, LaChaud G, Shen J, Asatrian G, Nguyen V, Zhang X, et al. A review of the clinical side effects of bone morphogenetic protein-2. Tissue Engineering Part B: Reviews. 2016;22(4):284-97.
76. Itoh K, Udagawa N, Katagiri T, Iemura S, Ueno N, Yasuda H, et al. Bone morphogenetic protein 2 stimulates osteoclast differentiation and survival supported by receptor activator of nuclear factor-κB ligand. Endocrinology. 2001;142(8):3656-62.
77. Jensen ED, Pham L, Billington CJ, Espe K, Carlson AE, Westendorf JJ, et al.

Bone morphogenic protein 2 directly enhances differentiation of murine osteoclast precursors. Journal of cellular biochemistry. 2010;109(4):672-82.
78. Abe E, Yamamoto M, Taguchi Y, Lecka-Czernik B, O'Brien CA, Economides AN, et al. Essential Requirement of BMPs-2/4 for Both Osteoblast and Osteoclast Formation in Murine Bone Marrow Cultures from Adult Mice: Antagonism by Noggin. Journal of Bone and Mineral Research. 2000;15(4):663-73.
79. Govender S, Csimma C, Genant H. Recombinant human bone morphogenetic protein-2 for treatment of open tibial fractures. Orthopedic Trauma Directions. 2010;8(05):31-7.
80. Pradhan BB, Bae HW, Dawson EG, Patel VV, Delamarter RB. Graft resorption with the use of bone morphogenetic protein: lessons from anterior lumbar interbody fusion using femoral ring allografts and recombinant human bone morphogenetic protein-2. Spine. 2006;31(10):E277-E84.
81. McKay WF, Peckham SM, Badura JM. A comprehensive clinical review of recombinant human bone morphogenetic protein-2 (INFUSE® Bone Graft). International orthopaedics. 2007;31(6):729-34.
82. Boyne PJ, Marx RE, Nevins M, Triplett G, Lazaro E, Lilly LC, et al. A feasibility study evaluating rhBMP-2/absorbable collagen sponge for maxillary sinus floor augmentation. The International journal of periodontics & restorative dentistry. 1997;17(1):11-25.
83. Boyne PJ, Lilly LC, Marx RE, Moy PK, Nevins M, Spagnoli DB, et al. De novo bone induction by recombinant human bone morphogenetic protein-2 (rhBMP-2) in maxillary sinus floor augmentation. Journal of Oral and Maxillofacial Surgery. 2005;63(12):1693-707.
84. Shahlaie K, Kim KD. Occipitocervical fusion using recombinant human bone morphogenetic protein-2: adverse effects due to tissue swelling and seroma. Spine. 2008;33(21):2361-6.
85. Robin BN, Chaput CD, Zeitouni S, Rahm MD, Zerris VA, Sampson HW. Cytokine-mediated inflammatory reaction following posterior cervical decompression and fusion associated with recombinant human bone morphogenetic protein-2: a case study. Spine. 2010;35(23):E1350-E4.
86. Epstein N. Complications due to the use of BMP/INFUSE in spine surgery: the evidence continues to mount. Surgical neurology international. 2013;4:343.
87. James AW, Zara JN, Zhang X, Askarinam A, Goyal R, Chiang M, et al. Perivascular stem cells: a prospectively purified mesenchymal stem cell population

for bone tissue engineering. Stem cells translational medicine. 2012;1(6):510-9.
88. Aghaloo T, Jiang X, Soo C, Zhang Z, Zhang X, Hu J, et al. A study of the role of nell-1 gene modified goat bone marrow stromal cells in promoting new bone formation. Molecular Therapy. 2007;15(10):1872-80.
89. Aryal R, Chen Xp, Fang C, Hu Yc. Bone Morphogenetic Protein-2 and Vascular Endothelial Growth Factor in Bone Tissue Regeneration: New Insight and Perspectives. Orthopaedic surgery. 2014;6(3):171-8.
90. Patel ZS, Young S, Tabata Y, Jansen JA, Wong ME, Mikos AG. Dual delivery of an angiogenic and an osteogenic growth factor for bone regeneration in a critical size defect model. Bone. 2008;43(5):931-40.
91. Kempen DH, Lu L, Heijink A, Hefferan TE, Creemers LB, Maran A, et al. Effect of local sequential VEGF and BMP-2 delivery on ectopic and orthotopic bone regeneration. Biomaterials. 2009;30(14):2816-25.
92. Michael W, Kino W, Francis M. Effectiveness of diphosphonates in preventing" osteoporosis" of disuse in the rat. Clinical orthopaedics and related research. 1971;78:271-6.
93. Lee K-B, Taghavi CE, Song K-J, Sintuu C, Yoo JH, Keorochana G, et al. Inflammatory characteristics of rhBMP-2 in vitro and in an in vivo rodent model. Spine. 2011;36(3):E149-E54.
94. Xiong C, Daubs MD, Montgomery SR, Aghdasi B, Inoue H, Tian H, et al. BMP-2 adverse reactions treated with human dose equivalent dexamethasone in a rodent model of soft-tissue inflammation. Spine. 2013;38(19):1640-7.
95. Herford AS, Boyne PJ. Reconstruction of mandibular continuity defects with bone morphogenetic protein-2 (rhBMP-2). Journal of Oral and Maxillofacial Surgery. 2008;66(4):616-24.
96. Martin Jr GJ, Boden SD, Morone MA, Moskovitz PA. Posterolateral intertransverse process spinal arthrodesis with rhBMP-2 in a nonhuman primate: important lessons learned regarding dose, carrier, and safety. Clinical Spine Surgery. 1999;12(3):179-86.
97. Kirker-Head CA. Potential applications and delivery strategies for bone morphogenetic proteins. Advanced drug delivery reviews. 2000;43(1):65-92.
98. Kim HD, Valentini RF. Retention and activity of BMP-2 in hyaluronic acid-based scaffolds in vitro. Journal of biomedical materials research. 2002;59(3):573-84.
99. Woo BH, Fink BF, Page R, Schrier JA, Jo YW, Jiang G, et al. Enhancement

of bone growth by sustained delivery of recombinant human bone morphogenetic protein-2 in a polymeric matrix. Pharmaceutical research. 2001;18(12):1747-53.

100. Liu T, Wu G, Wismeijer D, Gu Z, Liu Y. Deproteinized bovine bone functionalized with the slow delivery of BMP-2 for the repair of critical-sized bone defects in sheep. Bone. 2013;56(1):110-8.

101. Bessa PC, Casal M, Reis R. Bone morphogenetic proteins in tissue engineering: the road from laboratory to clinic, part II (BMP delivery). Journal of tissue engineering and regenerative medicine. 2008;2(2-3):81-96.

102. Arosarena OA, Collins WL. Bone regeneration in the rat mandible with bone morphogenetic protein-2: a comparison of two carriers. Otolaryngology-Head and Neck Surgery. 2005;132(4):592-7.

103. Fu YC, Nie H, Ho ML, Wang CK, Wang CH. Optimized bone regeneration based on sustained release from three-dimensional fibrous PLGA/HAp composite scaffolds loaded with BMP-2. Biotechnology and bioengineering. 2008;99(4):996-1006.

104. Rahman CV, Ben-David D, Dhillon A, Kuhn G, Gould TW, Müller R, et al. Controlled release of BMP-2 from a sintered polymer scaffold enhances bone repair in a mouse calvarial defect model. Journal of tissue engineering and regenerative medicine. 2014;8(1):59-66.

105. Yang HS, La W-G, Bhang SH, Jeon J-Y, Lee JH, Kim B-S. Heparin-conjugated fibrin as an injectable system for sustained delivery of bone morphogenetic protein-2. Tissue Engineering Part A. 2010;16(4):1225-33.

106. Li RH, Wozney JM. Delivering on the promise of bone morphogenetic proteins. Trends in biotechnology. 2001;19(7):255-65.

107. Moore WR, Graves SE, Bain GI. Synthetic bone graft substitutes. ANZ journal of surgery. 2001;71(6):354-61.

108. Schopper C, Moser D, Spassova E, Goriwoda W, Lagogiannis G, Hoering B, et al. Bone regeneration using a naturally grown HA/TCP carrier loaded with rh BMP-2 is independent of barrier-membrane effects. Journal of Biomedical Materials Research Part A. 2008;85(4):954-63.

109. Kim SS, Gwak SJ, Kim BS. Orthotopic bone formation by implantation of apatite-coated poly (lactide-co-glycolide)/hydroxyapatite composite particulates and bone morphogenetic protein-2. Journal of Biomedical Materials Research Part A. 2008;87(1):245-53.

110. Albee FH. Studies in bone growth: triple calcium phosphate as a stimulus to osteogenesis. Annals of surgery. 1920;71(1):32.
111. Jarcho M. Calcium phosphate ceramics as hard tissue prosthetics. Clinical orthopaedics and related research. 1981;157:259-78.
112. Geesink R, de Groot K, Klein C. Bonding of bone to apatite-coated implants. Bone & Joint Journal. 1988;70(1):17-22.
113. Byrd HS, Hobar PC, Shewmake K. Augmentation of the craniofacial skeleton with porous hydroxyapatite granules. Plastic and reconstructive surgery. 1993;91(1):15-22.
114. Yoneda M, Terai H, Imai Y, Okada T, Nozaki K, Inoue H, et al. Repair of an intercalated long bone defect with a synthetic biodegradable bone-inducing implant. Biomaterials. 2005;26(25):5145-52.
115. Horch H-H, Sader R, Pautke C, Neff A, Deppe H, Kolk A. Synthetic, pure-phase beta-tricalcium phosphate ceramic granules (Cerasorb®) for bone regeneration in the reconstructive surgery of the jaws. International journal of oral and maxillofacial surgery. 2006;35(8):708-13.
116. Hollinger JO, Brekke J, Gruskin E, Lee D. Role of bone substitutes. Clinical orthopaedics and related research. 1996;324:55-65.
117. Kwon SH, Jun YK, Hong SH, Lee IS, Kim HE, Won YY. Calcium phosphate bioceramics with various porosities and dissolution rates. Journal of the American Ceramic Society. 2002;85(12):3129-31.
118. Orii H, Sotome S, Chen J, Wang J, Shinomiya K. Beta-tricalcium phosphate (beta-TCP) graft combined with bone marrow stromal cells (MSCs) for posterolateral spine fusion. Journal of medical and dental sciences. 2005;52(1):51-7.
119. Cai S, Xu G, Yu X, Zhang W, Xiao Z, Yao K. Fabrication and biological characteristics of β-tricalcium phosphate porous ceramic scaffolds reinforced with calcium phosphate glass. Journal of Materials Science: Materials in Medicine. 2009;20(1):351-8.
120. Urist MR, Lietze A, Dawson E. [beta]-tricalcium Phosphate Delivery System for Bone Morphogenetic Protein. Clinical orthopaedics and related research. 1984;187:277-80.
121. Dohzono S, Imai Y, Nakamura H, Wakitani S, Takaoka K. Successful spinal fusion by E. coli-derived BMP-2-adsorbed porous β-TCP granules: a pilot study. Clinical Orthopaedics and Related Research®. 2009;467(12):3206-12.

122. Ohyama T, Yoshichika K, IWATA H, Waro T. β-Tricalcium phosphate combined with recombinant human bone morphogenetic protein-2: A substitute for autograft, used for packing interbody fusion cages in the canine lumbar spine. Neurologia medico-chirurgica. 2004;44(5):234-41.
123. Laffargue P, Hildebrand H, Rtaimate M, Frayssinet P, Amoureux J, Marchandise X. Evaluation of human recombinant bone morphogenetic protein-2-loaded tricalcium phosphate implants in rabbits' bone defects. Bone. 1999;25(2):55S-8S.
124. Glassman SD, Dimar JR, Carreon LY, Campbell MJ, Puno RM, Johnson JR. Initial fusion rates with recombinant human bone morphogenetic protein-2/compression resistant matrix and a hydroxyapatite and tricalcium phosphate/collagen carrier in posterolateral spinal fusion. Spine. 2005;30(15):1694-8.
125. Egermann M, Goldhahn J, Schneider E. Animal models for fracture treatment in osteoporosis. Osteoporosis international. 2005;16(2):S129-S38.
126. Cerroni AM, Tomlinson GA, Turnquist JE, Grynpas MD. Bone mineral density, osteopenia, and osteoporosis in the rhesus macaques of Cayo Santiago. American journal of physical anthropology. 2000;113(3):389-410.
127. Martin R, Butcher R, Sherwood L, Buckendahl P, Boyd R, Farris D, et al. Effects of ovariectomy in beagle dogs. Bone. 1987;8(1):23-31.
128. Newman E, Turner AS, Wark JD. The potential of sheep for the study of osteopenia: current status and comparison with other animal models. Bone. 1995;16(4 Suppl):277S-84S.
129. Seto H, Aoki K, Kasugai S, Ohya K. Trabecular bone turnover, bone marrow cell development, and gene expression of bone matrix proteins after low calcium feeding in rats. Bone. 1999;25(6):687-95.
130. Katsumata S-I, Matsuzaki H, Uehara M, Suzuki K. Effect of dietary magnesium supplementation on bone loss in rats fed a high phosphorus diet. Magnesium research. 2005;18(2):91-6.
131. Koshihara M, Masuyama R, Uehara M, Suzuki K. Effect of dietary calcium: Phosphorus ratio on bone mineralization and intestinal calcium absorption in ovariectomized rats. Biofactors. 2001;22(1-4):39-42.
132. Spencer G. Pregnancy and lactational osteoporosis. Animal model: porcine lactational osteoporosis. The American journal of pathology. 1979;95(1):277.

133. Lill C, Lill C, Fluegel A, Schneider E. Effect of ovariectomy, malnutrition and glucocorticoid application on bone properties in sheep: a pilot study. Osteoporosis International. 2002;13(6):480-6.
134. Chavassieux P, Buffet A, Vergnaud P, Garnero P, Meunier P. Short-term effects of corticosteroids on trabecular bone remodeling in old ewes. Bone. 1997;20(5):451-5.
135. Lelovas PP, Xanthos TT, Thoma SE, Lyritis GP, Dontas IA. The laboratory rat as an animal model for osteoporosis research. Comparative medicine. 2008;58(5):424-30.
136. Ducy P, Amling M, Takeda S, Priemel M, Schilling AF, Beil FT, et al. Leptin inhibits bone formation through a hypothalamic relay: a central control of bone mass. Cell. 2000;100(2):197-207.
137. Takeda S, Elefteriou F, Levasseur R, Liu X, Zhao L, Parker KL, et al. Leptin regulates bone formation via the sympathetic nervous system. Cell. 2002;111(3):305-17.
138. Gong J, Arnold J, Cohn S. Composition of trabecular and cortical bone. The Anatomical Record. 1964;149(3):325-31.
139. Bloebaum RD, Ota DT, Skedros JG, Mantas JP. Comparison of human and canine external femoral morphologies in the context of total hip replacement. Journal of Biomedical Materials Research Part A. 1993;27(9):1149-59.
140. Kimmel DB, Jee W. A quantitative histologic study of bone turnover in young adult beagles. The Anatomical Record. 1982;203(1):31-45.
141. Jee W, Yao W. Overview: animal models of osteopenia and osteoporosis. J Musculoskelet Neuronal Interact. 2001;1(3):193-207.
142. Lekholm U. Patient selection and preparation. Tissue-integrated prosthesis: osseointegration in clinical dentistry. 1985:199-209.
143. Hofbauer LC, Heufelder AE. The role of osteoprotegerin and receptor activator of nuclear factor κB ligand in the pathogenesis and treatment of rheumatoid arthritis. Arthritis & Rheumatism. 2001;44(2):253-9.
144. Bai Y-D, Yang F-S, Xuan K, Bai Y-X, Wu B-L. Inhibition of RANK/RANKL signal transduction pathway: a promising approach for osteoporosis treatment. Medical hypotheses. 2008;71(2):256-8.
145. Nam J-W, Kim M-Y, Han S-J. Cranial bone regeneration according to different particle sizes and densities of demineralized dentin matrix in the rabbit model. Maxillofacial Plastic and Reconstructive Surgery. 2016;38(1):27.

146. Kim IS, Lee EN, Cho TH, Song YM, Hwang SJ, Oh JH, et al. Promising efficacy of Escherichia coli recombinant human bone morphogenetic protein-2 in collagen sponge for ectopic and orthotopic bone formation and comparison with mammalian cell recombinant human bone morphogenetic protein-2. Tissue Engineering Part A. 2010;17(3-4):337-48.
147. Kim J, Kim IS, Cho TH, Kim HC, Yoon SJ, Choi J, et al. In vivo evaluation of MMP sensitive high-molecular weight HA-based hydrogels for bone tissue engineering. Journal of Biomedical Materials Research Part A. 2010;95(3):673-81.
148. Murphy CM, Schindeler A, Gleeson JP, Nicole Y, Cantrill LC, Mikulec K, et al. A collagen–hydroxyapatite scaffold allows for binding and co-delivery of recombinant bone morphogenetic proteins and bisphosphonates. Acta biomaterialia. 2014;10(5):2250-8.
149. Cho TH, Kim IS, Lee B, Park S-N, Ko J-H, Hwang SJ. Early and marked enhancement of new bone quality by alendronate-loaded collagen sponge combined with bone morphogenetic protein-2 at high dose: A long-term study in calvarial defects in a rat model. Tissue Engineering Part A. 2017.
150. Kim RY, Lee B, Park S-N, Ko J-H, Kim IS, Hwang SJ. Is Heparin Effective for the Controlled Delivery of High-Dose Bone Morphogenetic Protein-2? Tissue Engineering Part A. 2016;22(9-10):801-17.
151. Jo S, Kim S, Cho TH, Shin E, Hwang SJ, Noh I. Effects of recombinant human bone morphogenic protein-2 and human bone marrow-derived stromal cells on in vivo bone regeneration of chitosan–poly (ethylene oxide) hydrogel. Journal of Biomedical Materials Research Part A. 2013;101(3):892-901.
152. Park JC, Yu SB, Chung YI, Tae GY, Kim JJ, Park YD, et al. Bone regeneration with MMP sensitive hyaluronic acid-based hydrogel, rhBMP-2 and nanoparticles in rat calvarial critical size defect (CSD) model. Journal of the Korean Association of Oral and Maxillofacial Surgeons. 2009;35(3):137-45.
153. Kim H-C, Song J-M, Kim C-J, Yoon S-Y, Kim I-R, Park B-S, et al. Combined effect of bisphosphonate and recombinant human bone morphogenetic protein 2 on bone healing of rat calvarial defects. Maxillofacial plastic and reconstructive surgery. 2015;37(1):16.
154. Kwon T-K, Song J-M, Kim I-R, Park B-S, Kim C-H, Cheong I-K, et al. Effect of recombinant human bone morphogenetic protein-2 on bisphosphonate-treated osteoblasts. Journal of the Korean Association of Oral and Maxillofacial Surgeons. 2014;40(6):291-6.

155. Kelly MP, Vaughn OLA, Anderson PA. Systematic review and meta-analysis of recombinant human bone morphogenetic protein-2 in localized alveolar ridge and maxillary sinus augmentation. Journal of Oral and Maxillofacial Surgery. 2016;74(5):928-39.
156. Majid K, Tseng MD, Baker KC, Reyes-Trocchia A, Herkowitz HN. Biomimetic calcium phosphate coatings as bone morphogenetic protein delivery systems in spinal fusion. The Spine Journal. 2011;11(6):560-7.
157. Leknes KN, Yang J, Qahash M, Polimeni G, Susin C, Wikesjö UM. Alveolar ridge augmentation using implants coated with recombinant human bone morphogenetic protein-2: radiographic observations. Clinical oral implants research. 2008;19(10):1027-33.

TABLES

Table 1. Classification of implanted materials

	Implanted material
Implant	implant only
EXO-Inject	compound + implant
BMP5	BMP-2 5ug fused with compound + implant
BMP15	BMP-2 15ug fused with compound + implant
BMP45	BMP-2 45ug fused with compound + implant

Table 2. Micro-CT analysis of bone regeneration at the maxillary first molar extraction socket of beagle dogs in the control group (β-TCP microspheres with poloxamer hydrogel only) and the experimental group (45μg rhBMP-2 carried with β-TCP microspheres and poloxamer hydrogel)

	Control group	Experimental group	p - value
	Mean ± SD (mm)	Mean ± SD (mm)	
BV (mm^3)	2.49 ± 0.02	3.00 ± 0.04	<0.05
BV/TV (%)	33.29 ± 4.87	40.11 ± 7.42	<0.05
BSD (1/mm)	16.83 ± 0.79	17.69 ± 1.42	NS
Tb.Th.(mm)	0.07 ± 0.0001	0.09 ± 0.0002	NS
Tb.N. 1/mm)	4.45 ± 0.07	4.97 ± 0.06	<0.05
Tb.Sp.(mm)	0.12 ± 0.0001	0.12 ± 0.0001	NS

Values: means ± standard deviations

BV: Bone Volume, *BV/TV*: Bone Volume/Tissue Volume, percent bone volume, *BSD (Bone Surface Density)*: Bone volume/Tissue Volume, *Tb.Th*: Trabecular Thickness, *Tb.N*: Trabecular Number, *Tb.Sp*: Trabecular Separation

Table 3. Micro-CT analysis of RANKL- induced osteoporotic alveolar bone of the beagle dog mandible. Analysis was performed two weeks after the application of collagens soaked with RANKL 20ug, 40ug, 60ug and collagen only (control group).

	RANKL 20 ug	RANKL 40 ug	RANKL 60 ug	Collagen (n=3)
BV (mm^3)	28.51	14.08	13.11	24.1 ± 0.59
BV/TV (%)	46.9	23.16	21.57	39.65 ± 0.97
Tb.Th (mm)	0.87	0.52	0.57	0.67 ± 0.07
Tb.N (1/mm)	0.54	0.44	0.38	0.59 ± 0.05
Tb.Sp (mm)	1.69	2.47	2.67	1.92 ± 0.30

Values: means ± standard deviations

BV: Bone Volume, *BV/TV:* Bone Volume/Tissue Volume, percent bone volume, *BS:* Bone Surface, *BSD:* Bone Surface Density (BS/TV), *Tb.Th*: Trabecular Thickness, *Tb.N*: Trabecular Number, *Tb.Sp*: Trabecular Separation

Table 4. Comparison of the bone quality around the defect hole between the control and the all groups with RANKL application using micro-CT values immediately after the removal of collagen sponges with RANKL. The measurement method was illustrated in Fig. 4A

	Control	RANKL	*p*-value
BV/TV (%)	32.34±2.06	32.85±4.64	NS
Tb.Th. (mm)	0.09±0.01	0.12±0.03	NS
Tb.N. (1/mm)	3.50±0.30	2.88±0.59	NS
Tb.Sp. (mm)	0.11±0.01	0.17±0.04	NS
BMD (mg/cc)	1.37±0.01	1.37±0.02	NS

Values: means ± standard deviations

Table 5. Comparison of the bone quality around the defect holes (control; n = 6) with the bone quality at the outside of inter-thread space in all groups at 4 weeks (n = 2) and 6 weeks (n = 5) after implant placement using micro-CT. The measurement method was illustrated in figure 4A and 4B.

	Control	Implant			EXO-Inject			BMP5			BMP15			BMP45		
		4w	6w	Rate of increae (%)	4w	6w	Rate of increae (%)	4w	6w	Rate of increae (%)	4w	6w	Rate of increae (%)	4w	6w	Rate of increae (%)
BV/TV (%)	32.85 ± 4.64	30.99 ± 8.01	46.01 ± 4.97*	48.50 ± 17.56	32.98 ± 6.40	52.71 ± 4.88	59.82 ± 14.82	33.29 ± 6.95	57.67 ± 2.19	73.25 ± 6.57	26.25 ± 11.05	51.22 ± 7.19	84.41 ± 18.99	27.08 ± 10.84	52.29 ± 2.21	93.10 ± 8.16
Tb.Th. (mm)	0.12 ± 0.01	0.05 ± 0.01	0.07 ± 0.01	51.11 ± 16.62	0.04 ± 0.01	0.06 ± 0.01	45.00 ± 10.00	0.04 ± 0.02	0.06 ± 0.01	55.00 ±18.71	0.04 ± 0.02	0.06 ± 0.01	71.43 ± 20.20	0.04 ± 0.02	0.07 ± 0.01	81.25 ±10.83
Tb.N. (1/mm)	2.88 ± 0.26	8.02 ± 0.45	6.67 ± 0.75*	11.84 ± 9.74	8.68 ± 0.50	9.13 ± 1.34	5.27 ± 15.39	9.18 ± 1.63	9.78 ± 0.82	6.49 ± 8.95	6.96 ± 0.38	8.34 ± 1.17	18.32 ± 18.50	6.66 ± 0.28	7.75 ± 0.65	16.33 ± 9.80

Tb.Sp. (mm)	0.17 ± 0.02	0.07 ± 0.01	0.07 ± 0.01	5.71 ± 9.38	0.71 ± 0.01	0.06 ± 0.01	11.43 ±10.69	0.07 ± 0.02	0.05 ± 0.01	16.92 ± 7.54	0.07 ± 0.01	0.06 ± 0.01	20.00 ± 9.43	0.07 ± 0.01	0.06 ± 0.01	10.71 ± 11.85
BMD (mg/cc)	1.37 ± 0.01	1.38 ± 0.04	1.43 ± 0.02*	3.64 ± 1.97	1.39 ± 0.02	1.45 ± 0.03	4.03 ± 1.16	1.40 ± 0.03	1.47 ± 0.02	5.01 ± 1.91	1.31 ± 0.04	1.45 ± 0.02	10.68 ± 2.02	1.32 ± 0.03	1.45 ± 0.01	9.84 ± 2.15

Values: means ± standard deviation

Control: the bone quality around the defect holes immediately after the removal of RANKL

* $p<0.05$; Statistical analysis only between the control and the 6-weeks group due to the small number of cases in the 4-weeks group

Table 6. Comparison of the bone quality around the defect holes (control; n = 6) with the bone quality at the outside of inter-thread space in all groups with RANKL treatment (40 μg) at 4 weeks (n = 10) and 6 weeks after the removal of RANKL (n = 25) using micro-CT. The measurement method was illustrated in figure 4A and 4B.

	Control	4-weeks	6-weeks	Rate of increase 4w-6w (%)	*p*-value
BV/TV (%)	32.85 ± 4.64	30.64 ± 12.97	51.91 ± 6.75†, **	73.97 ± 18.24	<0.001
Tb.Th. (mm)	0.12 ± 0.01	0.04 ± 0.02††	0.07 ± 0.01†, *	61.90 ± 14.54	<0.001
Tb.N. (1/mm)	2.88 ± 0.26	7.70 ± 0.98†	8.46 ± 1.50†,	7.21 ± 11.03	<0.001
Tb.Sp. (mm)	0.17 ± 0.02	0.07 ± 0.01†	0.06 ± 0.04†	−11.07 ± 9.34	<0.05
BMD (mg/cc)	1.37 ± 0.01	1.36 ± 0.04	1.45 ± 0.03†, **	6.62 ± 1.72	<0.001

Values: means ± standard deviations

Control: the bone quality around the defect holes immediately after the removal of RANKL.

† $p < 0.05$ between the control and the 4 weeks group

†† $p < 0.001$ between the control and the 4 weeks group

‡ $p < 0.05$ between the control and the 6 weeks group

* $p < 0.05$ between the 4 weeks and the 6 weeks group

** $p < 0.001$ between the 4 weeks and the 6 weeks group

Table 7. Comparison of the bone regeneration within the inter-thread space/area between the 4 weeks (n = 2) and 6 weeks group (n = 5) in all groups using micro-CT and histomorphometric analysis (BA and BIC).

	Implant			EXO-Inject			BMP5			BMP15			BMP45		
	4w	**6w**	**Rate of increae (%)**	**4w**	**6w**	**Rate of increae (%)**	**4w**	**6w**	**Rate of increae (%)**	**4w**	**6w**	**Rate of increae (%)-**	**4w**	**6w**	**Rate of increae (%)**
BV/TV (%)	12.37 ± 0.02	14.80 ± 1.24	16.60 ± 10.01	13.52 ± 0.76	17.38 ± 1.52	28.55 ± 11.24	13.46 ± 0.64	16.48 ± 0.57	22.46 ± 8.42	12.21 ± 0.24	14.12 ± 1.77	15.62 ± 7.42	12.12 ± 0.90	14.37 ± 0.93	18.53 ± 15.26
Tb.Th. (mm)	0.05 ± 0.01	0.06 ± 0.01	12.60 ± 3.57	0.05 ± 0.01	0.06 ± 0.01	12.28 ± 7.97	0.05 ± 0.01	0.06 ± 0.01	14.79 ± 11.50	0.05 ± 0.01	0.05 ± 0.01	5.21 ± 6.02	0.05 ± 0.01	0.05 ± 0.01	11.64 ± 8.31
Tb.N. (1/mm)	2.56 ± 0.14	2.72 ± 0.34	6.22 ± 3.17	2.72 ± 0.01	3.15 ± 0.25	15.87 ± 9.06	2.78 ± 0.27	2.94 ± 0.06	5.53 ± 4.16	2.49 ± 0.09	2.74 ± 0.69	9.94 ± 5.73	2.51 ± 0.16	2.65 ± 0.14	5.31 ± 7.45

Tb.Sp. (mm)	0.69 ± 0.03	0.73 ± 0.01	5.08 ± 1.39	0.71 ± 0.01	0.0.74 ± 0.03	4.24 ± 4.55	0.69 ± 0.02	0.73 ± 0.01	5.63 ± 2.10	0.70 ± 0.01	0.72 ± 0.02	2.88 ± 1.42	0.69 ± 0.03	0.72 ± 0.01	4.16 ± 1.44
BMD (mg/cc)	1.27 ± 0.01	1.30 ± 0.01	2.49 ± 1.97	1.29 ± 0.01	1.34 ± 0.01	4.09 ± 1.36	1.28 ± 0.00	1.33 ± 0.01	3.37 ± 1.11	1.27 ± 0.01	1.29 ± 0.01	2.09 ± 1.02	1.27 ± 0.01	1.30 ± 0.01	2.55 ± 2.15
BA (%)	34.51 ± 0.05	44.05 ± 5.43	14.07 ± 14.09	42.23 ± 0.43	51.97 ± 4.64	23.43 ± 11.03	43.80 ± 1.40	58.50 ± 6.30	33.55 ± 14.38	40.65 ± 7.45	56.88 ± 4.77	31.93 ± 11.74	45.65 ± 3.55	54.54 ± 3.59	19.46 ± 7.88
BIC (%)	39.46 ± 2.79	50.05 ± 5.21	29.74 ± 13.51	42.12 ± 8.26	58.1 ± 4.22	37.99 ± 10.01	50.34 ± 1.17	66.56 ± 12.65	51.97 ± 18.88	43.30 ± 9.58	57.40 ± 9.07	38.55 ± 16.89	35.13 ± 17.23	52.45 ± 4.56	14.89 ± 9.99

No statistical analysis due to the small number of case in the 4 weeks group.

Table 8. Comparison of the bone regeneration within the inter-thread space/area between the 4 weeks (all cases; n = 10) and 6 weeks group (all cases; n = 25) using micro-CT and histomorphometric analysis (BA and BIC) independent on the group classification according to the bone graft materials in Table 1.

	4-weeks	6-weeks	Rate of increase (%)	*p*-value
BV/TV (%)	12.73 ± 0.62	15.10 ± 1.93	20.36 ± 4.72	<0.001
Tb.Th. (mm)	0.05 ± 0.01	0.06 ± 0.01	11.30 ± 3.22	<0.001
Tb.N. (1/mm)	2.61 ± 0.12	2.77 ± 0.25	8.57 ± 4.01	<0.05
Tb.Sp. (mm)	0.70 ± 0.01	0.73 ± 0.01	4.40 ± 0.94	<0.001
BMD (mg/cc)	1.27 ± 0.01	1.31 ± 0.02	2.92 ± 0.72	<0.001
BA (%)	40.17 ± 5.34	53.03 ± 7.18	25.51 ± 15.15	<0.001
BIC (%)	42.07 ± 9.87	56.92 ± 9.69	36.28 ± 12.05	<0.05

Values: means ± standard deviations

Table 9. Comparison of 4 weeks and 6 weeks increase rate (%) between inside and outside of inter-thread space/area in all groups using micro-CT.

	Implant			EXO-Inject			BMP5			BMP15			BMP45		
	Inside	**Outside**	***p*-value**	**Inside**	**Outside**	***p*-value**	**Inside**	**Outside**	***p*-value**	**Inside**	**Outside**	***p*-value**	**Inside**	**Outside**	***p*-value**
BV/TV (%)	16.60 ± 10.01	48.50 ± 17.56	<0.05	28.55 ± 11.24	59.82 ± 14.82	<0.05	22.46 ± 8.42	73.25 ± 6.57	<0.05	15.62 ± 7.42	84.41 ± 10.84	<0.05	18.53 ± 15.26	93.10 ± 8.16	<0.05
Tb.Th. (mm)	12.60 ± 3.57	51.11 ± 16.62	<0.05	12.28 ± 7.97	45.00 ± 10.00	<0.05	14.79 ±11.50	55.00 ± 18.71	<0.05	5.21 ± 6.02	71.43 ± 20.20	<0.05	11.64 ± 8.31	81.25 ± 10.83	<0.05
Tb.N. (1/mm)	6.22 ± 3.17	−11.84 ± 9.74	ns	15.87 ± 9.06	5.27 ± 15.39	ns	5.53 ± 4.16	6.49 ± 8.95	ns	9.94 ± 5.73	18.32 ± 18.50	ns	5.31 ± 7.45	16.33 ± 9.80	ns
Tb.Sp. (mm)	5.08 ± 1.39	5.71 ± 9.38	ns	4.24 ± 4.55	−11.43 ± 10.69	<0.05	5.63 ± 2.10	−16.92 ± 7.54	<0.05	2.88 ± 1.42	−20.00 ± 9.43	<0.05	4.16 ± 1.44	−10.71 ± 11.85	<0.05

BMD (mg/cc)	2.49 ± 1.97	3.64 ± 1.97	ns	4.09 ± 1.36	4.03 ± 1.16	ns	3.37 ± 1.11	5.01 ± 1.91	<0.05	2.09 ± 1.02	10.68 ± 2.02	<0.05	2.55 ± 2.15	9.84 ± 2.15	<0.05

Values: means ± standard deviations

Table 10. Micro-CT analysis of peri-implant bone regeneration 4 weeks (n=2) after implant placement in different doses of rhBMP-2 carried with β-TCP microspheres and poloxamer hydrogel in RANKL-induced local osteoporotic alveolar bone of the beagle dog mandible.

	Implant	**EXO -Inject**	**BMP5**	**BMP15**	**BMP45**
BV/TV (%)	18.58 ± 4.42	16.43 ± 3.20	18.37 ± 3.12	15.63 ± 4.38	17.95 ± 2.38
Tb.Th (1/mm)	0.05 ± 0.01	0.05 ± 0.01	0.05 ± 0.01	0.05 ± 0.01	0.06 ± 0.02
Tb.N (1/mm)	3.47 ± 0.08	3.36 ± 0.10	3.91 ± 0.48	3.14 ± 0.17	3.61 ± 0.92
Tb.Sp (mm)	0.52 ± 0.05	0.51 ± 0.03	0.51 ± 0.05	0.51 ± 0.01	0.53 ± 0.02
BMD (mg/cm^3)	1.39 ± 0.04	1.36 ± 0.03	1.39 ± 0.02	1.35 ± 0.05	1.38 ± 0.02

Values: means ± standard deviations, BV: Bone Volume, BV/TV: Bone Volume/Tissue Volume, percent bone volume, BSD: Bone Surface Density, Bone surface/Tissue volume, Tb.Th: Trabecular Thickness, Tb.N: Trabecular Number, Tb.Sp: Trabecular Separation, BMD: Bone Mineral Density

No statistical analysis due to the small number of case in the 4 weeks group.

Table 11. Micro-CT analysis of peri-implant bone regeneration 6 weeks (n=5) after implant placement in different doses of rhBMP-2 carried with β-TCP microspheres and poloxamer hydrogel in RANKL-induced local osteoporotic alveolar bone of the beagle dog mandible.

	Implant	**EXO-Inject**	**BMP5**	**BMP15**	**BMP45**	***p*-value**
BV/TV (%)	23.14 ± 1.78	26.23 ± 0.65*	27.22 ± 1.53*†	23.13 ± 0.89	22.97 ± 0.95	<0.05
Tb.Th (1/mm)	0.08 ± 0.01†	0.08 ± 0.01	0.08 ± 0.01	0.08 ± 0.01	0.10 ± 0.01	NS
Tb.N (1/mm)	2.82 ± 0.28	3.21 ± 0.15*†	3.46 ± 0.32†	2.90 ± 0.34	2.48 ± 0.26	<0.05
Tb.Sp (mm)	0.58 ± 0.02	0.58 ± 0.02	0.57 ± 0.03	0.56 ± 0.01†	0.58 ± 0.01	NS
BMD (mg/cm^3)	1.43 ± 0.02	1.47 ± 0.01	1.49 ± 0.03*	1.43 ± 0.01	1.44 ± 0.01	<0.05

Values: means ± standard deviations, *: significant difference compared with Implant group ($p < 0.05$), †: significant difference compared with BMP45 group ($p<0.05$). BV: Bone Volume, BV/TV: Bone Volume/Tissue Volume, percent bone volume, BSD: Bone Surface Density, Bone surface/Tissue volume, Tb.Th: Trabecular Thickness, Tb.N: Trabecular Number, Tb.Sp: Trabecular Separation, BMD: Bone Mineral Density

Table 12. Histomorphometric analysis of the peri-implant bone regeneration 4 weeks (n=2) after implant placement in different doses of rhBMP-2 carried with β-TCP microspheres and poloxamer hydrogel in RANKL-induced local osteoporotic alveolar bone of the beagle dog mandible.

	Implant	**EXO-Inject**	**BMP5**	**BMP15**	**BMP45**
BA (%)	34.51 ± 0.05	42.23 ± 0.43	43.80 ± 1.40	40.65 ± 7.45	39.65 ± 3.55
BIC (%)	39.46 ± 2.79	42.12 ± 8.26	50.34 ± 1.17	43.30 ± 9.58	35.13 ± 17.23

Values: means ± standard deviations, BA: bone area (%), BIC: bone implant contact (%)

No statistical analysis due to the small number of case in the 4 weeks group.

Table 13. Histomorphometric analysis of the peri-implant bone regeneration 6 weeks (n=5) after implant placement in different doses of rhBMP-2 carried with β-TCP microspheres and poloxamer hydrogel in RANKL-induced local osteoporotic alveolar bone of the beagle dog mandible.

	Implant	**EXO-Inject**	**BMP5**	**BMP15**	**BMP45**	***p*-value**
BA (%)	44.05 ± 5.43	51.97 ± 4.64*	58.49 ± 6.30*	56.88 ± 4.77	54.53 ± 3.59	<0.05
BIC (%)	50.05 ± 4.63	58.10 ± 3.78*	66.56 ± 5.98*†‡	57.40 ± 8.06	52.44 ± 4.63	<0.05

Values: means ± standard deviations, *: statistical significance compared to Implant group ($p<0.05$), †: statistical significance compared to EXO-Inject group ($p<0.05$), ‡: statistical significance compared to BMP45 group ($p<0.001$), BA: bone area (%), BIC: bone implant contact (%)

Figures and Figure legends

A)

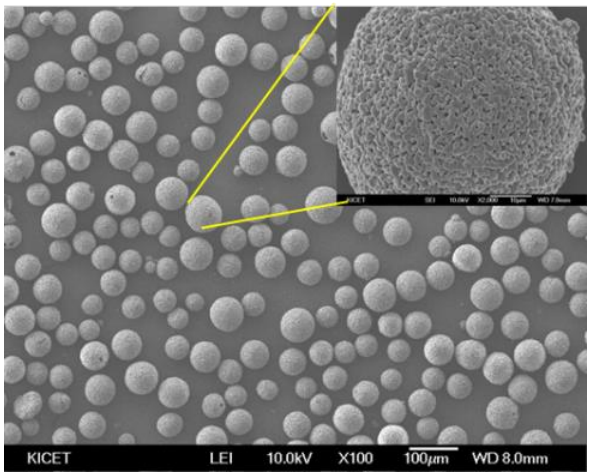

B)

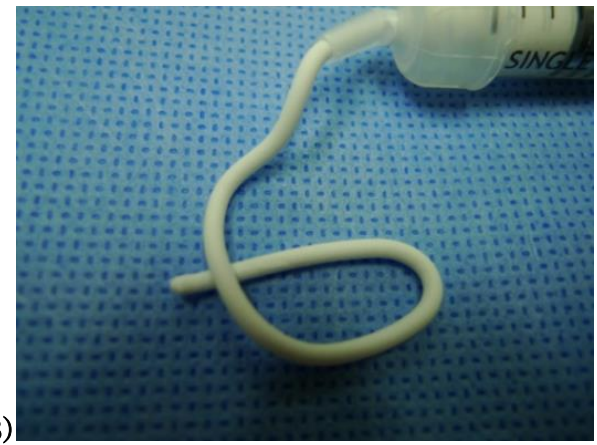

Figure 1. A) SEM images of β-TCP microspheres generated by the spray-dry method after sintering at 1,050℃. The β-TCP microsphere had a porosity of 68 % and particle size of 45~75 μm, B) injectable β-TCP microspheres bone graft material consisting of porous β-TCP microspheres and poloxamer hydrogel.

A)

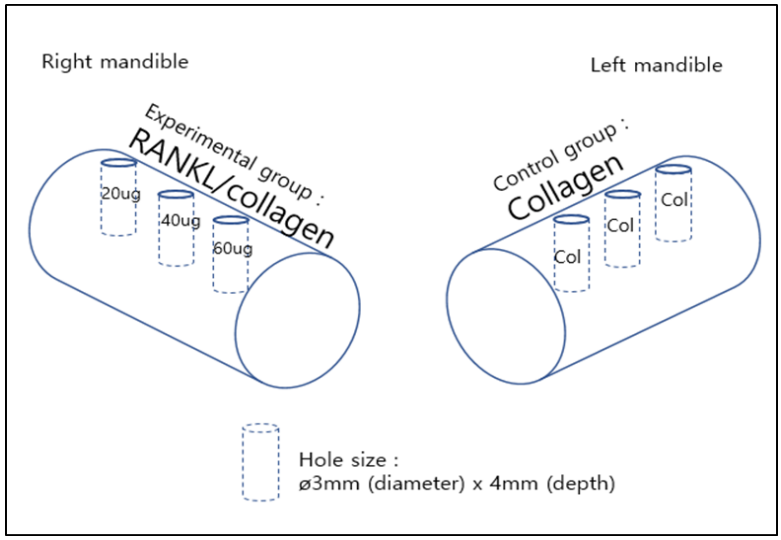

B)

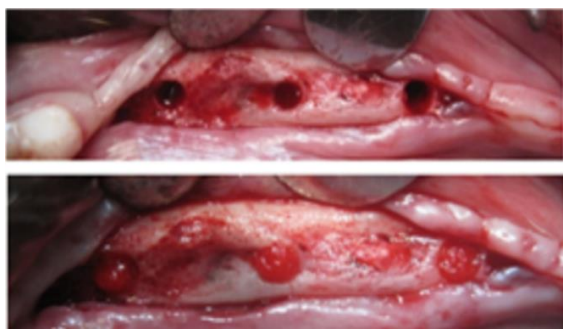

Figure 2. Schematic illustration of the local osteoporotic set-up model (A) and perioperative photographs (B). Holes (3 mm in diameter, 4 mm in depth) were made, and collagen sponges containing RANKL with different concentrations (20, 40, and 60 μg) were applied to the holes in the experimental group. Collagen sponges without RANKL were applied to the holes in the control group. Animal experiment for RANKL-induced local osteoporotic alveolar bone model of the beagle dog mandible. *Col*: collagen.

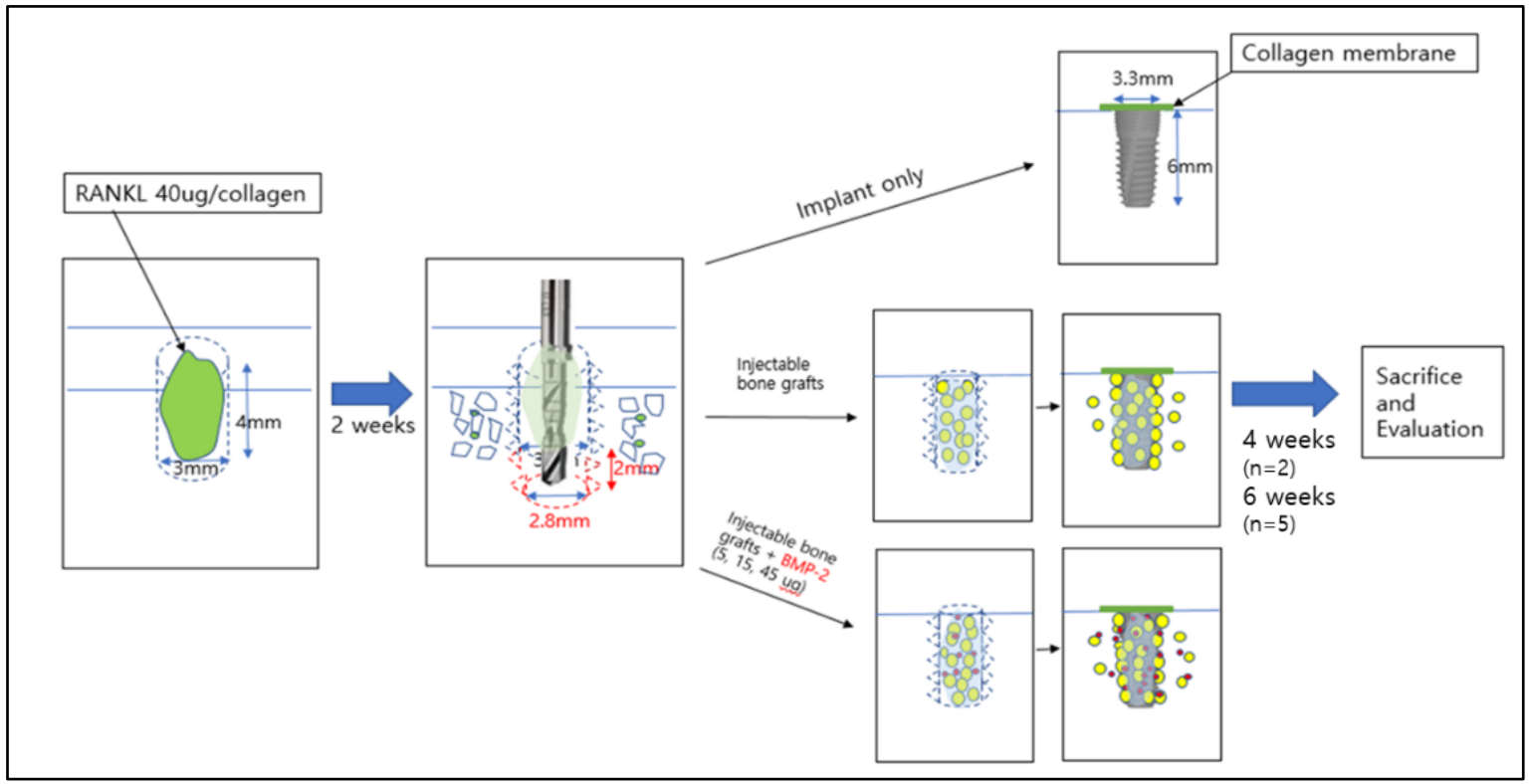

Figure 3. Schematic illustration of the implant placement model. A collagen sponge with 40 μg of

absorbed RANKL was positioned in the hole for two weeks to create a local osteoporosis model. After the removal of collagen sponge, the hole was further drilled for 2 mm in depth with a twist drill (2.8 mm in diameter) for stable initial implant fixation (6 mm long implant). Implants were placed in the drilled holes with and without the injectable bone grafts in five groups. Animals were sacrificed four weeks (n=2) six weeks (n=5) after dental implant placement for the evaluation of peri-implant bone formation. B) Five groups were placed on each mandible of beagles (n=7). Implant-only and EXO-Inject were placed in the right side and BMP5, BMP15 and BMP45 groups were placed on left side. The distance between the groups was 10 mm at the center of each implant. The dental implant fixture is 3.3 mm in diameter and 6 mm in length , and have the SLA treated surface.

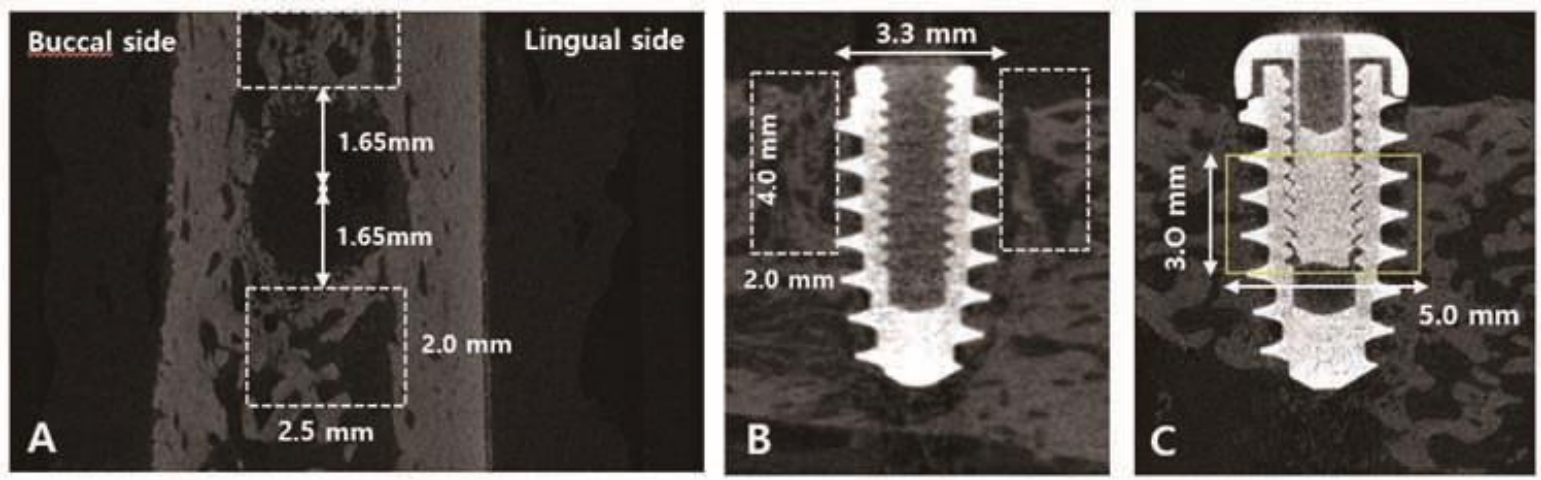

Figure 4. Micro-CT analysis to evaluate the changes of bone quality around the defect hole after the removal of RANKL-collagen sponge (A) and the peri-implant new bone formation at four and six weeks after implant placement (B, C). The changes immediately after the removal of RANKL were measured in the local osteoporotic set-up model (A), and the changes four and six weeks after the removal of RANKL were evaluated in the implant placement models (B). The size of VOI in A and B was 2.5 mm in buccolingual depth, 2 mm in anteroposterior width and 4 mm in height

from the alveolar crest in the local osteoporotic set-up model and from the upper margin of implant in the implant model. The inner border was distanced 1.65 mm from the center of the hole in the local osteoporotic set-up model and from the center of the dental implant (3.3 mm in diameter) in the implant model. The VOI in C included the peri-implant space with a diameter of 5 mm from the second to fifth thread, which corresponded with approximately 3 mm in height, and 350 slices from the second thread. VOI: volume of interest

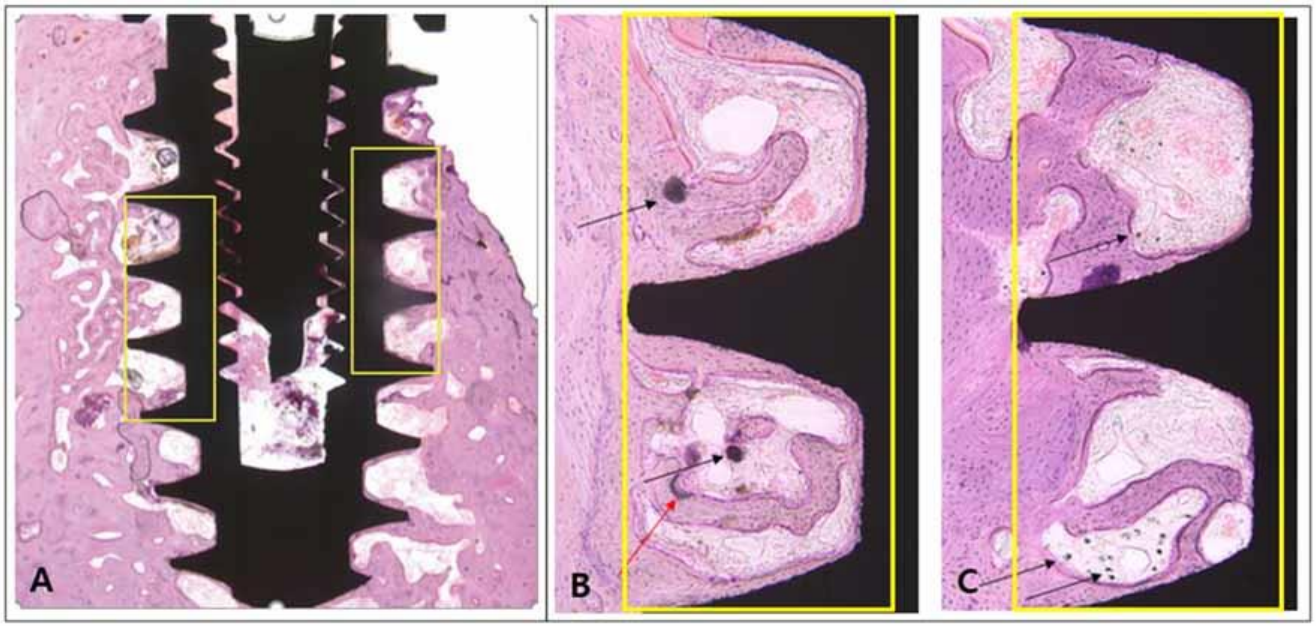

Figure 5. Reference area for the histomorphometric analysis (A) and residual β-TCP microspheres in the histology (B, C). The bone area (BA) and total area were measured within the inter-thread area from the second to the fifth thread crests on both sides of the implant. For the bone implant contact (BIC) measurements, the length of implant surface with bone contact and the total length

between the second and the fifth thread crest on both sides of the implant were measured (A). β-TCP microspheres in hematoxylin-eosin stained undecalcified sections six weeks after implant placement. A tiny amount of unabsorbed (black arrows) and resorbing particles (red arrow) was observed in the EXO-Inject group (B), and the size was more reduced in the BMP15 group (C). These were not distinguished from the new bone on micro-CT images. Magnification: x 100. *BA*: bone area, *BIC*: bone-to-implant contact.

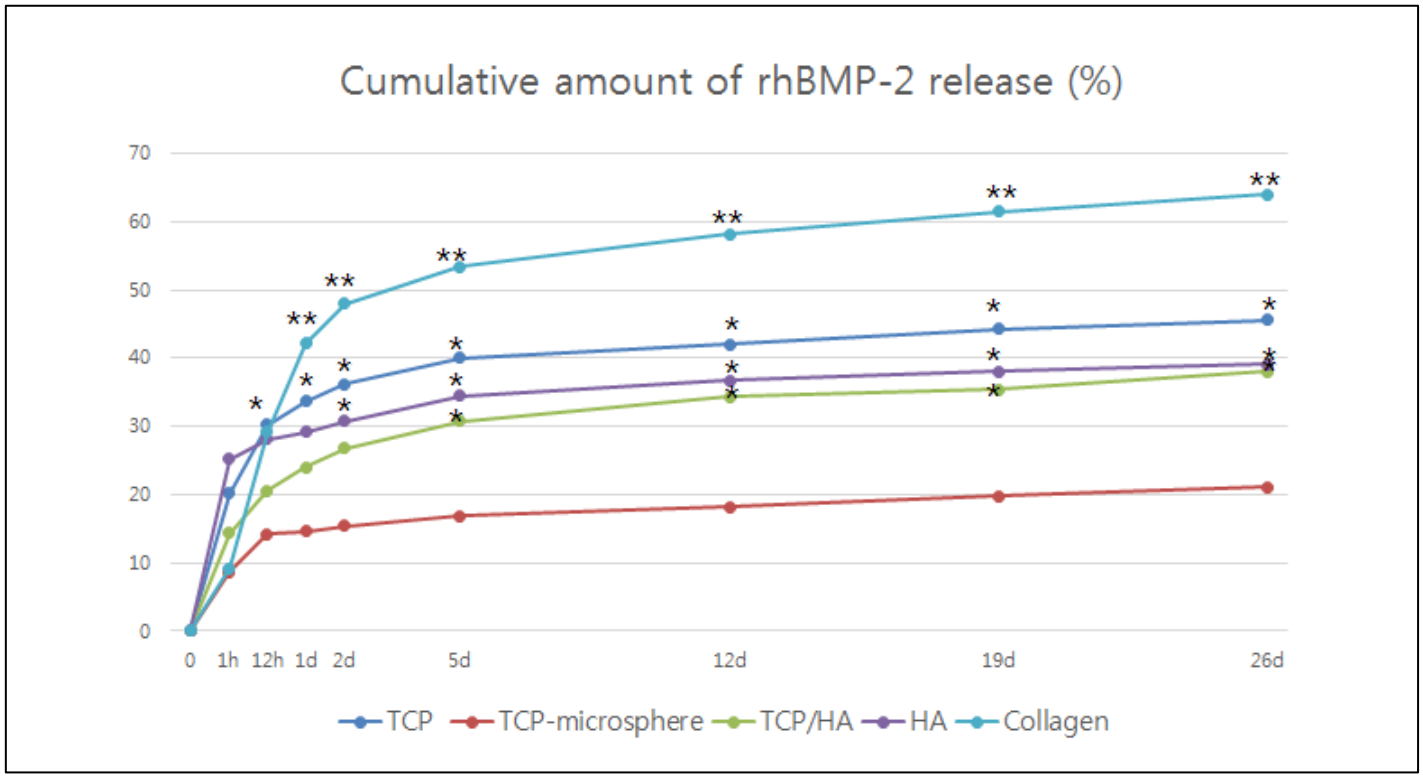

Figure 6. Sustained release of rhBMP-2 by 5 different carriers in vitro. β-TCP microsphere showed significantly more sustained release compared to the collagen sponge ($p<0.05$ at 12h,

p<0.001 at 1d, 2d, 5d, 12d, 19d and 26d), TCP granules (p<0.05 at 1d, 2d, 5d, 12d, 19d and 26d), HA (p<0.05 at 2d, 5d, 12d, 19d and 26d) and biphasic calcium phosphate (TCP/HA) (p<0.05 at 5d, 12d, 19d and 26d).

β-TCP: 100% β-tricalcium phosphate granule, HA: 100% hydroxy apatite granule, TCP-microsphere: porous β-TCP microsphere, TCP/HA: Biphasic calcium phosphate (70%TCP + 30%HA) granule, Collagen: Collagen sponge, *: p<0.05, **p<0.001

A) 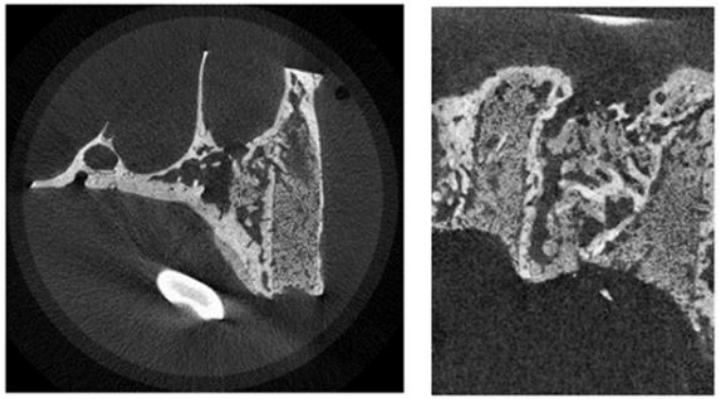 B) 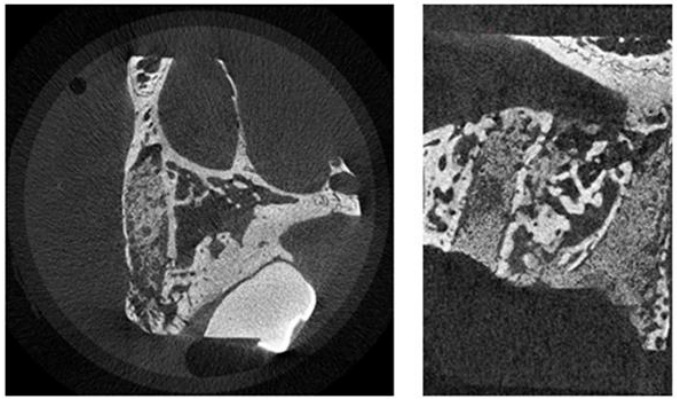

Figure 7. Micro-CT images of bone regeneration by β-TCP microspheres with poloxamer hydrogel only (A: the control group) and with 45μg rhBMP carried with β-TCP microspheres with poloxamer hydrogel (B: the experimental group) at the maxillary first molar extraction socket of beagle dogs. Images on sagittal (left picture) and coronal plane (right picture)

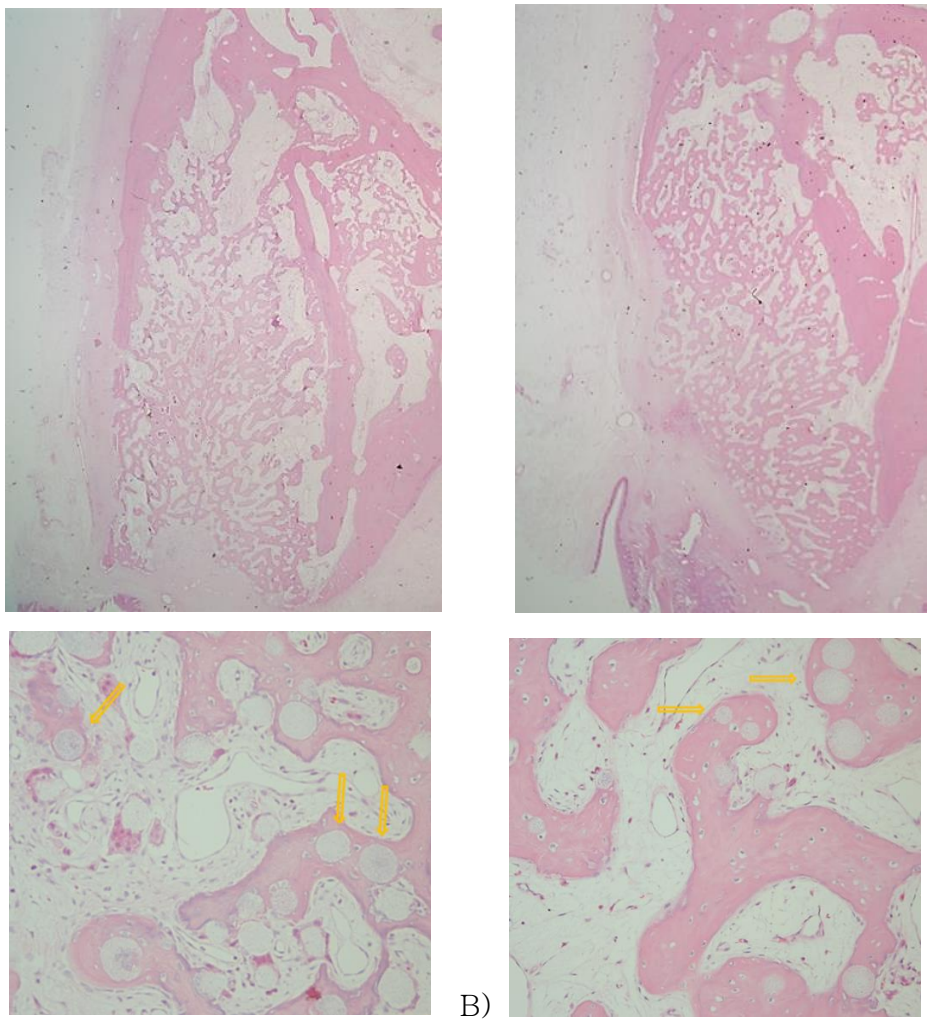

Figure 8. Histological images of bone regeneration at the maxillary first molar extraction sockets of beagle dogs in the control group (A; β-TCP microspheres with poloxamer hydrogel only) and the experimental group (B: 45μg rhBMP-2 carried with β-TCP microspheres and poloxamer hydrogel). Some β-TCP microspheres were unabsorbed remained in the center of extraction sockets in both groups. In the experimental group, the unabsorbed β-TCP microspheres were fully embedded by newly formed trabecular bone, while there were some unabsorbed β-TCP

microspheres not surrounded by new bone in the control group. Stained with hematoxylin and eosin. The image magnifications were x12.5 (upper pictures) and x200 (lower pictures).

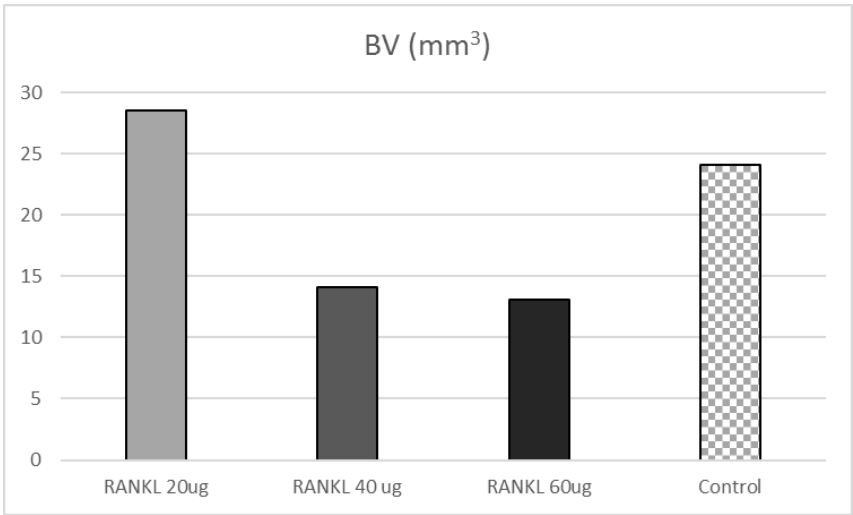

Figure 9. Evaluation of the osteoporotic change by the measurement of bone volume (BV) after the application of collagen sponges soaked with RANKL (20, 40 and 60 μg) and only collagen (control group) for two weeks in the local osteoporotic set-up model. In groups treated with RANKL (40 and 60 μg), the BV was clearly reduced. BV: bone volume.

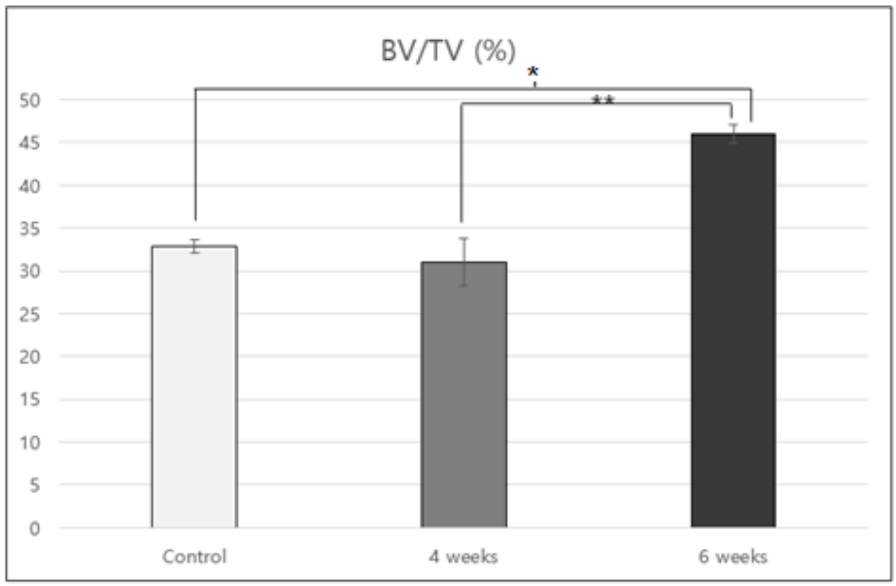

Figure 10. Comparison of the bone quality on the mesial and distal side of defect holes (control; n = 6)) in the local osteoporotic set-up model with it on the mesial and distal side of inter-thread space at 4-weeks (n = 10) and 6- weeks after the removal of RANKL (n = 25) using micro-CT, when all cases in the same waiting period were classified into a same group, independent of the use of injectable graft material and the concentration of rhBMP-2 in Table 1. The measurement method was illustrated in Fig. 4A, B. There was no significant difference between the control and the 4-weeks. The BV/TV at 6-weeks was significantly increased compared to it in the 4-weeks group. * $p < 0.05$, ** $p<0.001$

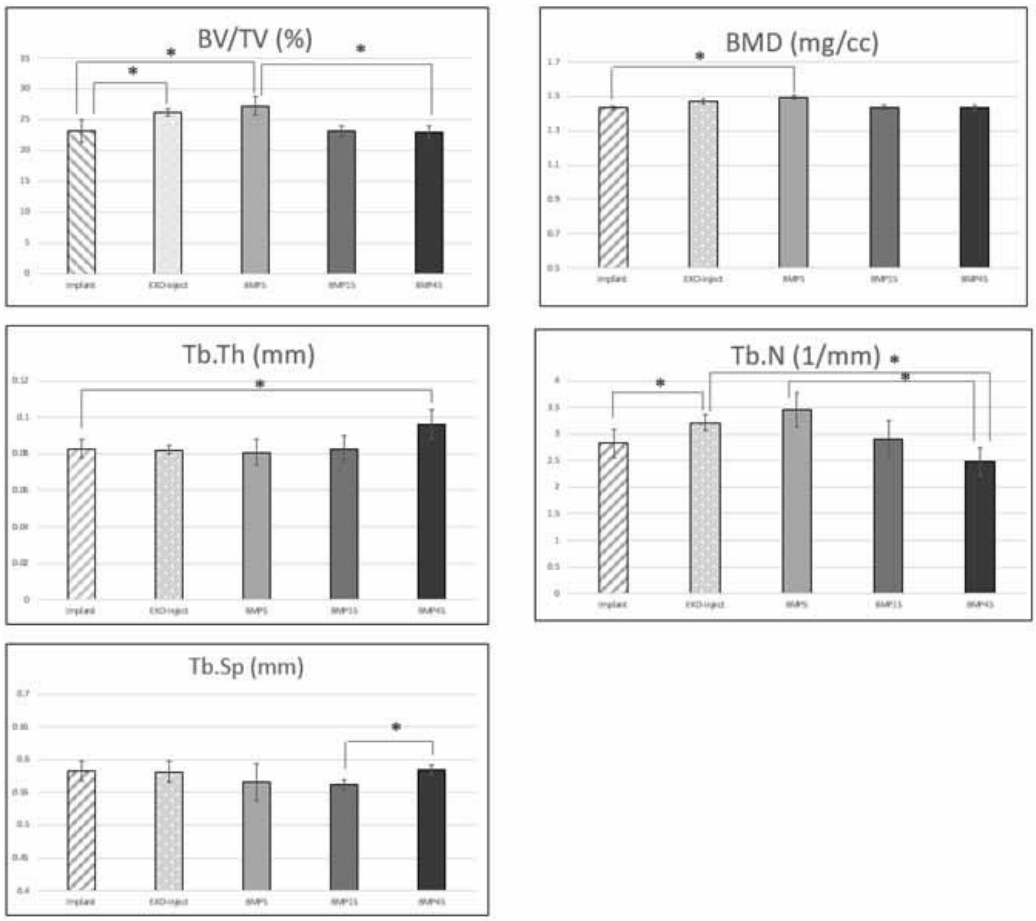

Figure 11. 3D micro-CT analysis of peri-implant bone regeneration at 6-weeks in different doses of rhBMP-2 carried with β-TCP microspheres and poloxamer hydrogel in RANKL-induced local osteoporotic alveolar bone of the beagle dog mandible. Compared to the Implant only group, the BV/TV was significantly higher in the BMP 5 and EXO-Inject group ($p<0.05$), however, it was lower in the BMP15 and BMP45 group. There was no significant difference of the BV/TV between the BMP 5 and EXO-Inject group.

BV: bone volume, BV/TV: bone volume/tissue volume, BMD: bone mineral density, Tb.Th: trabecular thickness, Tb.N: trabecular number, Tb.Sp: trabecular space. *: $p<0.05$

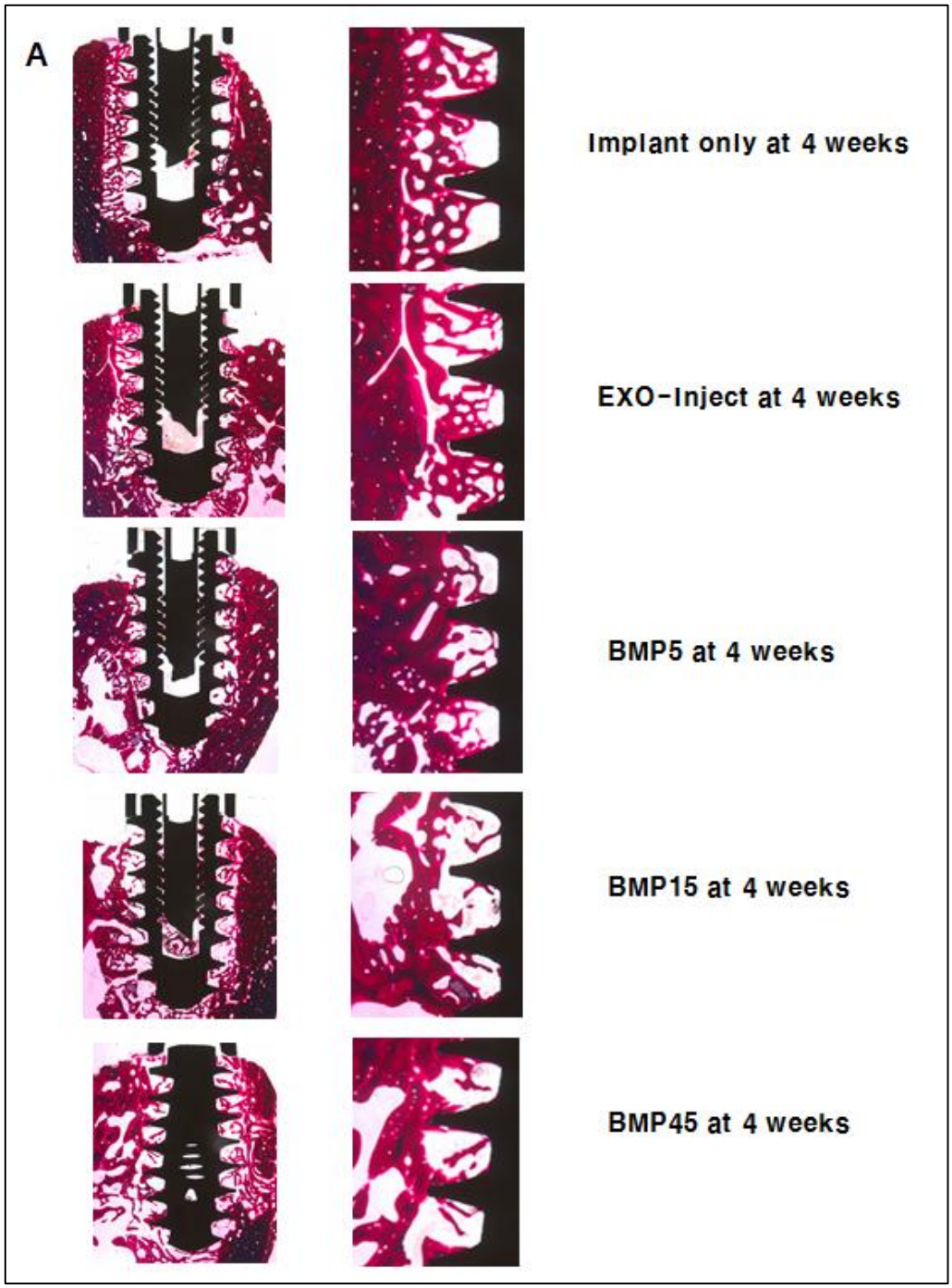
A
Implant only at 4 weeks
EXO-Inject at 4 weeks
BMP5 at 4 weeks
BMP15 at 4 weeks
BMP45 at 4 weeks

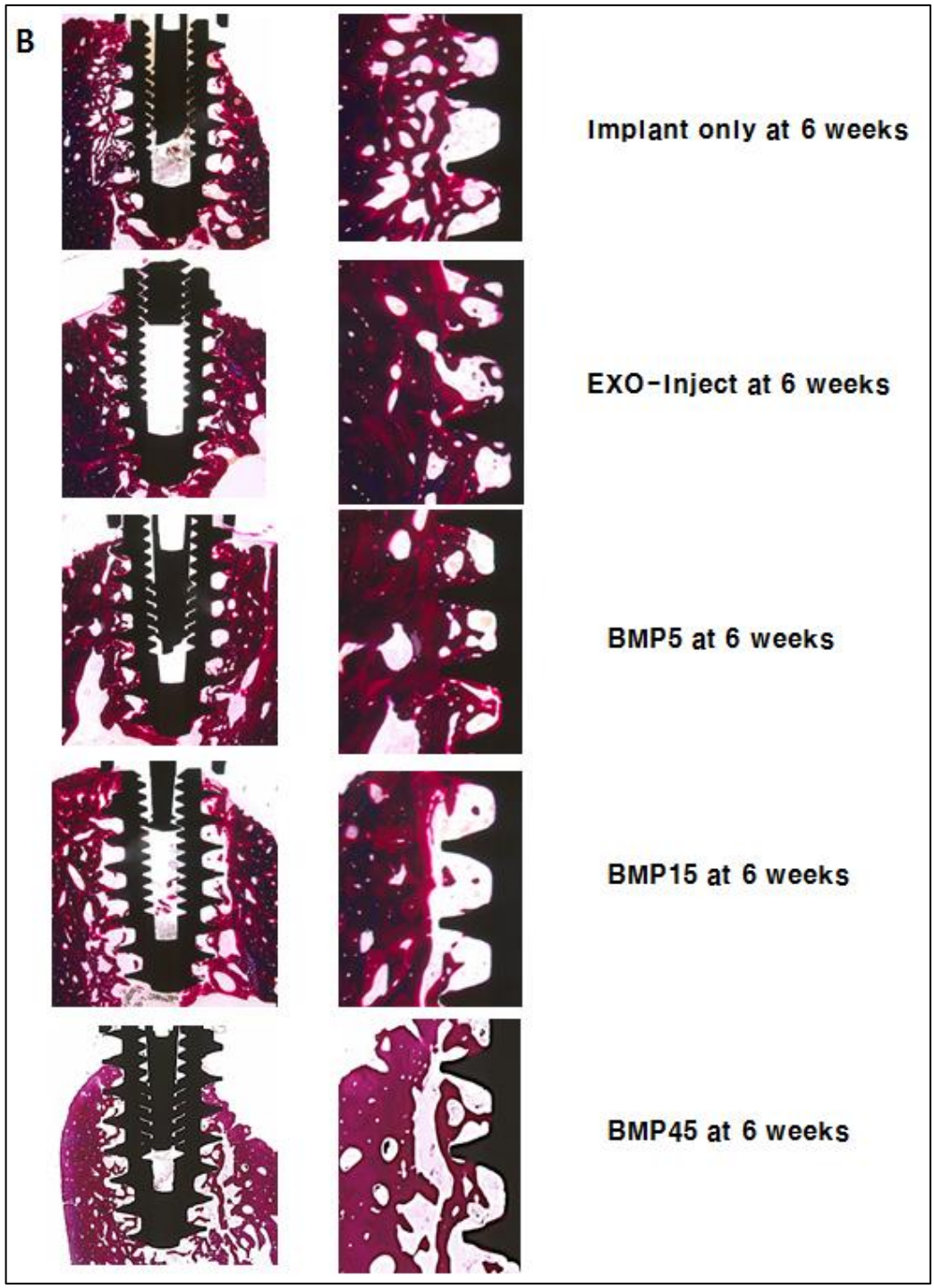
B
Implant only at 6 weeks
EXO-Inject at 6 weeks
BMP5 at 6 weeks
BMP15 at 6 weeks
BMP45 at 6 weeks

Figure 12. Histological images of the peri-implant bone regeneration in different doses of rhBMP-2 carried with β-TCP microspheres and poloxamer hydrogel in RANKL-induced local osteoporotic alveolar bone of the beagle dog mandible 4 weeks (A) and 6 weeks after implant placement (B). Undecalcified sections (50-μm thickness). Image magnifications on the left side: x 12.5, it on the right side: x 40. Compared to the image at 4 weeks (A), the bone formation was clearly increased at the outside of thread crests at 6 weeks, while it was slightly increased within the inter-thread area (first image in B)

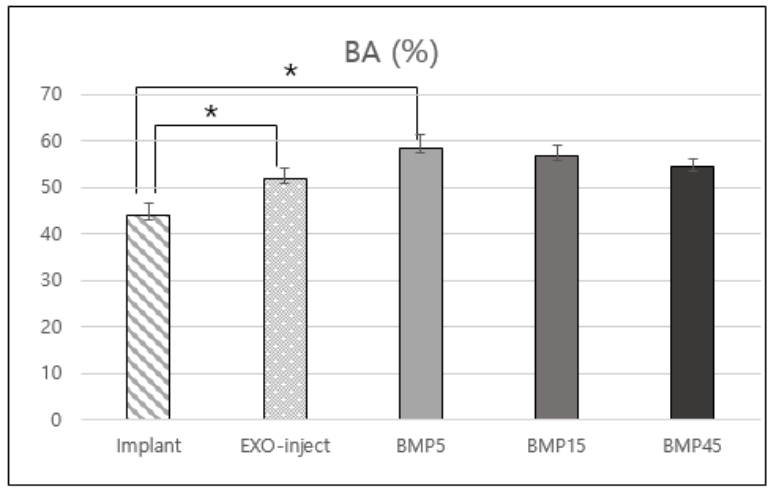

A)

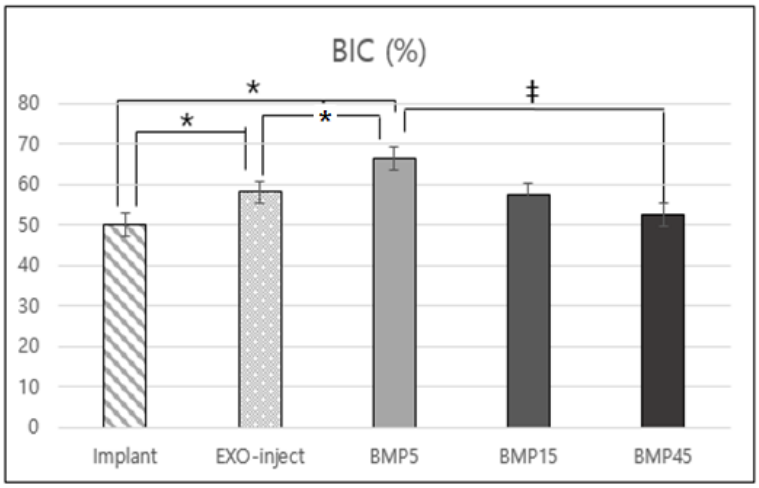

B)

Figure 13. Histomorphometric analysis of the peri-implant bone regeneration at 6-weeks in different doses of rhBMP-2 carried with β-TCP microspheres and poloxamer hydrogel in RANKL-induced local osteoporotic alveolar bone of the beagle dog mandible. The bone area (BA) (%) was obtained from the ratio of BA/total area within the inter-thread area (A), and the bone-implant-contact (BIC) was calculated from the ration of bone

contact length/total length (B). The BA and BIC were significantly higher in the EXO-Inject and BMP5 groups compared to the Implant only group. The BMP5 group showed a significantly higher BIC than the EXO-Inject, while there was no significant difference of BA between two groups. *: $p<0.05$, ǂ: $p<0.001$.

-국문 초록-

핵인자카파-B 활성화수용체리간드로 유도된 국소적 골다공증을 동반한 비글견 치조골 모델에서 골형성 단백질을 함유한 주사형 베타-삼칼슘인산 미세구의 골형성 효과에 대한 연구

장 아 렴

서울대학교 대학원 치의과학과 구강악안면외과학 전공

(지도교수 황 순 정)

1. 배 경: 장시간의 치유 시간 후에도 치과용 임플란트와 치조골 사이의 충분한 골 유착을 얻지 못하는 불량한 골질을 가진 환자들을 위한 치과 임플란트 수요가 증가되고 있다. 제2형 골형성단백질 (BMP-2)과 같은 뼈형성촉진성장인자의 사용은 골다공증성 치조골에서 임플란트 주변 골을 강화시켜 임플란트 성공률을 높일 수 있다. 이러한 결과를 얻기 위해서는 서방형 rhBMP-2 방출 특성을 가지고, 주사형에 적합한 작은 입자 크기를 가진 새로운 캐리어가 필요하다. 개의 하악골은 치과임플란트와 골이식재에 대한 골재생연구에 적합한 대동물로 간주되고 있지만, 골다공증을 동반한 개의 치조골 모델은 아직 개발되지 못했다.

2. 목 적:

본 연구의 목적은 핵인자카파-B활성화수용체리간드(RANKL)를 국소적으로 적용하여 치조골에서의 국소적 골다공성 모델을 개발하고, 다공성 베타-삼칼슘인산 미세구의 rhBMP-2 방출속도를 조사하고, 국소적 골다공증을 동반한 치조골에서 다공성 베타-삼칼슘인산미세구와 폴록사머 하이드로겔로 구성된 주사형 골이식재를 rhBMP-2와 혼합하여 사용하는 새로운 주사형 골이식재를 평가함에 있다.

2. 방 법:

다공성 β-TCP 미세구의 BMP-2 (5μg/ml) 서방성을 현재 골이식재로 많이 사용되는 과립형 골이식재들 (100 % 수산화인회석 (HA), 100% 베타 삼칼슘인산 (TCP), 2상 인산 칼슘 (70 % TCP + 30 % HA)) 및 콜라겐 스폰지와 비교하였다. 동물 실험에서, rhBMP-2 (45μg)를 함유하거나 함유하지 않은 다공성 β-TCP 미세구와 폴록사머 하이드로겔 혼합물을 4마리 비글의 양측 상악 제1대구치의 발치와에 이식하였다. 4 주 후, 비글견들을 희생시키고, 상악 제 1 대구치를 포함하는 각 실험 부위를 채취 하여, 골 재생 평가를 위한 미세컴퓨터단층촬영 (micro-CT) 분석 및 조직학적 분석을 시행하였다.

국소적 골다공증을 동반한 개의 하악 치조골 모델을 개발하기 위하여, 비글견의 하악골에 직경 3mm, 깊이 4mm의 홀을 만들어, 20μg, 40μg, 60μg RANKL이 흡수된 콜라겐 스폰지를 2주간 적용한 후, micro-CT 분석을 통한 골질

평가를 토대로 설계하여 최대 골다공증성 골질을 위한 RANKL 용량을 확립하였다, 일곱 마리의 비글견 하악 치조골에서 위의 실험에서 결정된 용량의 RANKL을 2주간 적용하여 국소적 골다공증의 치조골을 만든 후, RANKL이 흡수된 콜라겐 스폰지를 제거하고, 임플란트만을 식립하거나(대조군) 4가지 BMP-2 농도(0, 5, 15, 45 μg)를 함유한 주사형 β-TCP미세구 골이식재를 홀에 주입하고 임플란트를 식립하고 4주(n = 2)와 6주(n = 5) 후에 동물을 안락사시키고 micro-CT와 조직형태학적 분석을 통해 나사산 사이공간의 외측에서의 골질 변화와 나사산 사이공간의 내측에서의 골재생을 평가하였다.

3. 결 과:

BMP-2의 서방속도 조사에서, 다공성 β-TCP미세구는 다른 과립형 전달체보다 유의하게 BMP-2의 서방 방출을 하였으며($p < 0.05$), 콜라겐 스폰지에 비해서는 12시간에 이후에 보다 느리게 방출을 하였다($p < 0.001$). 총 방출량은 마지막 관찰 (26일째)에 적용된 총량의 21% 였다. 동물실험에서는, 골체적 (BV), 전체조직에 대한 골체적의 비율 (BV/TV), 해면골 수 (trabecular number) 값이 BMP-2를 함유하지 않은 대조군에서 보다 BMP-2를 함유한 실험군에서 통계적으로 유의하게 높았다 ($p<0.05$).
치조골에서 국소적 골다공증을 유도하는 RANKL의 농도는 40 μg이었으며, BV은 RANKL 40 μg에서 RANKL을 적용하지 않은 대조군과 비교하여 41.61 % 감소했다. 나사산 사이공간 외측에서의 BV/TV은, RANKL 제거

직후(32.85%)보다 4주 후(30.64%)에 약간 더 감소하였다. 그러나 6 주 후의 BV/TV(51.91%)과 BMD(1.45 mg/cc)는 4 주 경과한 후의 BVTV(30.64%)과 BMD(1.36 mg/cc)에 비해 유의하게 증가 하였다. 나사산 사이공간 내측에서의 골질변화 비교 분석에서, 6주에서의 모든 micro-CT 변수들은 4주에서의 변수보다 유의하게 높았다. 4주에서의 나사산 사이공간 내측의 BV/TV (12.73%), BMD (1.27 mg/cc) 그리고 조직계측에서의 BA (40.17%)는 6주에 각각 15.10%, 1.31mg/cc 그리고 53.03%로 유의하게 증가하였다($p < 0.001$). 하지만 나사산 사이공간 내측에서의 증가비율은 나사산 사이공간 외측에서의 증가비율에 비해 작았다.

그룹별 임프란트 주변 골재생 평가에서, 임플란트 식립 4주후에는, 임프란트만 식립한 군과 rhBMP-5를 투여 한 군에서 가장 높은 BV/TV (18.58 %, 18.37 %) 와 BMD (1.39 mg / cc, 1.39 mg / cc)를 보였고, 통계적으로 유의하지는 않았다. 6 주 후 평가에서는, 5μg BMP-2를 함유한 β-TCP 골이식재 그룹이 가장 높은 BV / TV (27.22 %)를 보였으며, 이는 임플란트만 식립한 대조군(23.14%)과 45μg BMP-2를 함유한 군(22.97%) 보다 통계적으로 유의하게 높은 수치였다($p < 0.05$). 골이식재만 주입한 군에서의 BV/TV(26.23%)는 임플란트만 식립한 대조군에서 보다 유의하게 높았다($p < 0.05$).
4주 조직형태학적 분석에서, 5 μg BMP-2를 함유한 β-TCP 골이식재 군에서 BA(43.80%)와 골임플란트접촉(BIC)

(50.34%)가 가장 높았다. 6주에서의 BA와 BIC는, 임플란트만 식립한 대조군(44.05%, 50.05%)에서 보다 골이식재만 사용한 군(51.97%, 58.10%)과 5 μg BMP-2를 함유한 골이식재(58.49%, 66.56%)에서 유의하게 높았다($p < 0.05$). 6주에 골이식재만 주입한 군과 5 μg BMP-2를 함유한 골이식재를 주입한 군에서 BA의 차이는 없었지만, BIC는 5 μg BMP-2를 함께 사용한 군(66.56%)에서 골이식재만 주입한 군 (58.10%)과($p < 0.05$) 45 μg BMP-2를 함께 사용한 군(52.44%)에 비해 ($p<0.001$) 유의하게 높았다.

4. 결 론:

다공성 베타-삼칼슘인산미세구와 폴록사머 하이드로겔로 구성된 새로운 주사형 골이식재는 BMP-2를 서방하고 쉽게 BMP-2를 즉시 혼합하고 용이하게 사용할 수 있는 특성이 있어서 향상된 골재생을 가져 올 수 있겠다고 판단된다. 본 연구를 통해 40 μg RANKL을 콜라겐스폰지에 적혀서 치조골에 형성된 홀에 2주간 적용하여 하악 치조골의 국소적 골다공증 모델을 개발하였다. 개발된 국소적 골다공증의 시간 변화에 따른 골질 변화 평가에서, 임플란트 나사산 사이공간 외측의 4주 골질은 RANKL제거 직후 보다 조금 더 감소하였지만, 6주에서는 많이 증가하였고, 임플란트 나사산 사이공간 내측의 6주 골질은 4주에 비해서는 유의하게 높았다. 전체적으로 보아 치조골에서 40 μg RANKL로 유도된 국소적 골다공증은 4주까지는 잘 지속된다고 판단된다.

주사형 다공성 베타-삼칼슘인산미세구 골이식재를 국소적 골다공증 모델에서 효과적으로 평가할 수 있었으며, 5 μg BMP-2를 함께 사용하면 다른 군에 비해서 가장 좋은 임플란트주위 신생골이 형성되었고, BMP-2의 용량이 이보다 더 높아져도 신생골의 형성은 증가되지 않았다. 본 연구에서 개발된 치조골의 국소적 골다증증 모델은 골다공증을 가진 노년층 환자의 골형성 촉진을 위한 임플란트 표면과 골이식재 개발에 유용하게 활용할 수 있을 것으로 판단된다.

주요어: 베타-삼칼슘인산미세구, 제2형골형성단백질, 서방 방출, 국소적 골다공증성 치조골, 핵인자카파-B리간드의수용체활성화제, 임플란트주변골재생